# Design of a Wide Range kVp-meter

by

**Murat Tümer**

BS, in Electrical Engineering, Boğaziçi University, 2004

Submitted to the Institute of Biomedical Engineering
in partial fulfillment of the requirements
for the degree of
Master of Science
in
Biomedical Engineering

Boğaziçi University
June 2007

**Design of a Wide Range kVp-meter**

**APPROVED BY:**

Prof. Yekta Ülgen .....
(Thesis Advisor)

Prof. Mehmed Özkan .....

Prof. Yani Skarlatos .....

**DATE OF APPROVAL:** June 12, 2007

# ACKNOWLEDGMENTS

I dedicate this work to my family for their pecuniary and moral support since my birth, which made this work possible and because we have always been a good and happy family.

I am very thankful to Prof. Yekta Ülgen for his guidance throughout my thesis. Without his guidance and support, this work would not be possible.

I gratefully acknowledge Prof. Mehmed Özkan for his intellectual contribution to this study by asking interesting questions and letting me to think more detailed. I would also like to thank Prof. Yani Skarlatos for attending my thesis defense and his crucial comments.

A special thank goes to ASM biomedical staff, for their permission to use the X-ray unit and to Mr. Basri Durmuşoğlu for manufacturing the lead case for photodiodes.

# ABSTRACT

## Design of a Wide Range kVp-meter

The kVp setting is one of the major factors affecting the image quality in X-ray imaging and should be annually measured and calibrated if necessary. In this thesis, a kVp-meter is designed and a prototype unit was built and the performance was tested in terms of accuracy and reliability. The design is based on the dependency of the attenuation coefficient of metals on the energy of the incident photons, which is related to kVp. The tests on the prototype showed that the accuracy and precision are both below 1% in the diagnostic range. As the same measuring principle applies for mammography unit, this device can be also used for kVp measurements of mammography units. The accuracy and precision in the mammography mode are below 1%, too.

**Keywords:** kilovolts peak, X-ray, photodiode, copper filter, linear attenuation coefficient, calibration.

# ÖZET

## Geniş Bant bir kVp-metre Tasarımı

Röntgen görüntülerinin kalitesini belirleyen faktörlerden biri olan kVp ayarı her yıl mutlaka ölçülmeli ve standartlara göre %5'ten büyük bir sapma varsa yeniden kalibre edilmelidir. Bu çalışmada bir kVp-metre tasarlanmış ve prototipi üretilmiş, daha sonra da çalışması kesinlik, duyarlık ve güvenlilirlik açısından denenmiştir. Tasarlanırken metallerin gelen fotonların enerjileri ile, bir anlamda da röntgen tüpünün kVp'si ile değişen geçirgenliğinden yararlanılmıştır. Bu prototip üzerinde yapılan ölçümlerde iyi sonuçlar elde edilmiştir. Kesinlik ve duyarlık sapmalarının %1'in altında olduğu tespit edilmiştir. Tanısal radyolojide kullanılan bu ölçüm presibi mamografi cihazlarında da geçerli olduğundan cihaz mamografi kVp'lerinin ölçümünde de kullanılabilmektedir. Mamografi kipinin ölçüm kesinliği ve duyarlığının da %1'in altında olduğu ölçülmüştür.

**Anahtar Sözcükler:** kilovolt peak, röntgen ışını, fotodiyot, bakır süzgeç, doğrusal zayıflatma katsayısı, kalibrasyon

# TABLE OF CONTENTS

# LIST OF FIGURES

# LIST OF TABLES

# LIST OF SYMBOLS

| | |
|---|---|
| $D$ | Dose |
| $I$ | Intensity of the X-ray beam |
| $V_{BE}$ | Base-emitter voltage |
| $I_C$ | Collector current |
| $V_T$ | Thermal voltage |
| $I_S$ | Saturation current |
| | |
| $\mu$ | Linear attenuation coefficient |
| $\omega$ | Coherent scattering coefficient |
| $\tau$ | Photoelectric absorption coefficient |
| $\sigma$ | Compton scattering coefficient |
| $\kappa$ | Pair production coefficient |
| $\pi$ | Photodisintegration coefficient |

# LIST OF ABBREVIATIONS

| | |
|---|---|
| kVp | Kilovoltage peak |
| kVe | Kilovoltage effective |
| HVL | Half Value Layer |
| SID | Source-to-image distance |
| ADC | Analog-to-digital converter |
| BJT | Bipolar junction transistor |
| IC | Integrated circuit |

# 1. INTRODUCTION

One of the requirements of the quality assurance program in the hospitals is the annual measurement of the peak kilovoltage (kVp) setting of X-ray devices, because kVp contributes directly to image formation and dose absorbed by the patient [3], [5].

The kVp control of the X-ray device is a measure for the energy level of the emitted X-rays and corresponds to the penetrating power of the beam. To increase the contrast on the radiographic image, the kVp should be adjusted according to the type of the tissue. For example, if bone is examined, a relatively low kVp (60kVp) is applied. But if the lung tissue is suspected, then a higher kVp in the range of 110 to 130 is used. Also, the body size of the patient is also important factor in deciding the kVp level. The kVp affects not only the intensity reaching the image receptor but also the subject contrast of the image. An uncalibrated X-ray machine leads to unnecessary exposure of the patients. For this reason, the kVp adjusting circuit of the X-ray machines should be controlled on regular basis. The error range is given as $\pm 5\%$ [6]. There are various ways to measure the kVp; each will be considered briefly.

1. **Invasive or direct method:** In this method, a voltage divider tank is used. The voltage divider divides the voltage to a measurable low range. Then, by measuring this relatively small voltage the exact value is calculated. It is also possible to track the waveform by using an oscilloscope [7]. This method, being invasive, is difficult to put into practice and also dangerous for the technician [6]. However, it is the most accurate method and treated as the reference standard [8].

2. **Non-invasive or indirect methods:**

   - X-ray Spectrometer: In this method, the X-ray spectrum is measured using an X-ray spectrometer and the highest energy photons refer to the highest kV, namely kVp [9]. Another approach is to find the peak value of the output spectrum, which corresponds to the kVe (effective kilovoltage) and use this

kVe information to calculate the peak kilovoltage [5].

The main drawback of the method is the need for an expensive X-ray spectrometer. Corrections are necessary to find the actual spectrum [9].

- kVp Test Cassettes: These cassettes provide a good measurement of the peak tube potential. On the cassette there are two columns of holes. Both are exposed and the X-ray is filtered by a copper sheet to remove the low energy photons before they reach the holes. Then one column of the holes is covered and filtered by a copper wedge which produces a series of circles of decreasing intensity on the film. The second column of the holes is not filtered by any additional copper sheet or wedge, but the light produced by the screen is partly transmitted to the film by an optical attenuator. These circles produced on the film are of equal density and serve as reference. The kVp is easily found by comparing the densities of the adjacent circles [10, 11]. The main drawbacks of this method are the time required to develop the film and the number of films that are wasted.

- Another method, consists in measuring the ratio of the intensities of two X-ray beams after passing metal filters of known thicknesses (Figure 1.1). This ratio contains the information on the peak kilo-voltage used to accelerate the electrons in the tube.

  Figure 1.2 shows the dependence of the linear attenuation coefficient on the energy level of the photons [1]. This implies that, when the attenuation coefficient can be measured then the energy level of the photons hence the kVp can be calculated. This is the idea behind the commercially available non-invasive kVp-meter designs.

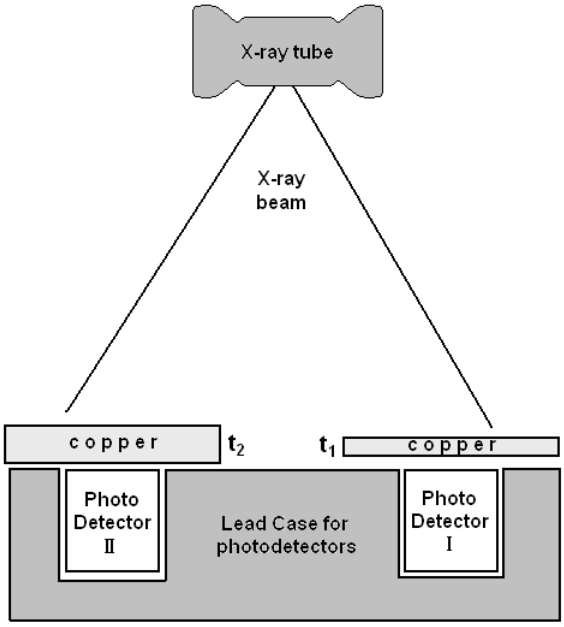


**Figure 1.1** The x-ray beam passes two metal filters of different thicknesses and different signal levels detected at the photodetectors.

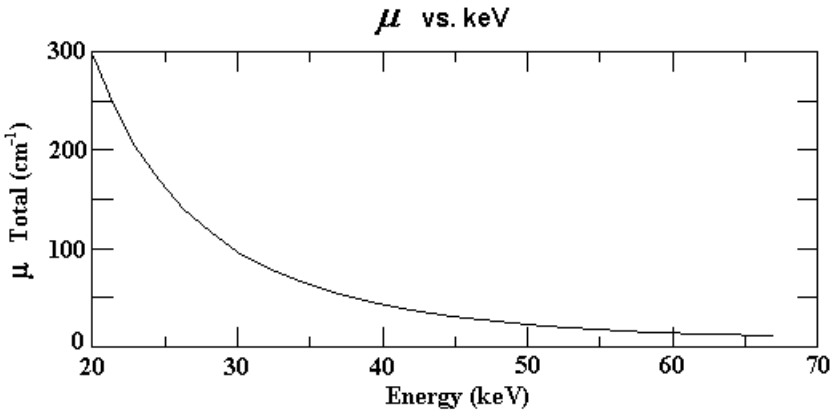


**Figure 1.2** The relation between the linear attenuation coefficient of copper and the incident photon energy [1].

# 2. THEORY and METHOD

## 2.1 X-ray Generation

X-ray was the name given to these highly penetrating rays by their German discoverer Wilhelm Röntgen. They are high frequency electromagnetic rays which are radiated when high energy electrons strike a metal target. There are two processes leading to X-ray photons:

- X-ray photons are emitted when high speed electrons are suddenly decelerated due to attraction with the positively charged target atom nuclei. - these rays are called *Bremsstrahlung radiation*, or "braking radiation". The Bremsstrahlung photons have a continuous energy spectrum as seen in Figure 2.2.

- X-ray photons are also emitted when electrons make transitions between lower atomic energy levels in heavy elements. X-rays produced in this way have definite energies just like other line spectra from atomic electrons. They are called *characteristic X-rays* since they have energies determined by the atomic energy levels. The energy spectrum of this type of radiation is discrete, as seen in Figure 2.2). Since the first energy level of an atom is called K-shell, the X-rays produced by transitions from the $n = 2 \rightarrow n = 1$ levels are called $K_\alpha$ X-rays, and those for the $n = 3 \rightarrow n = 1$ transition are called $K_\beta$ X-rays [2]. These radiations are similar to Lyman-$\alpha$ and Lyman-$\beta$ series of hydrogen atom.

The electrons freed from the heated filament are accelerated by the high voltage between the cathode and anode and focused to the target by the focusing cup. The amount of the freed electrons per a given time interval, namely the number of the electrons hitting the target, is determined by the mA setting of the tube and linearly related to the beam intensity. The target is made usually of tungsten (diagnostic X-ray machines) due to its high atomic number, which increases the efficiency in X-ray

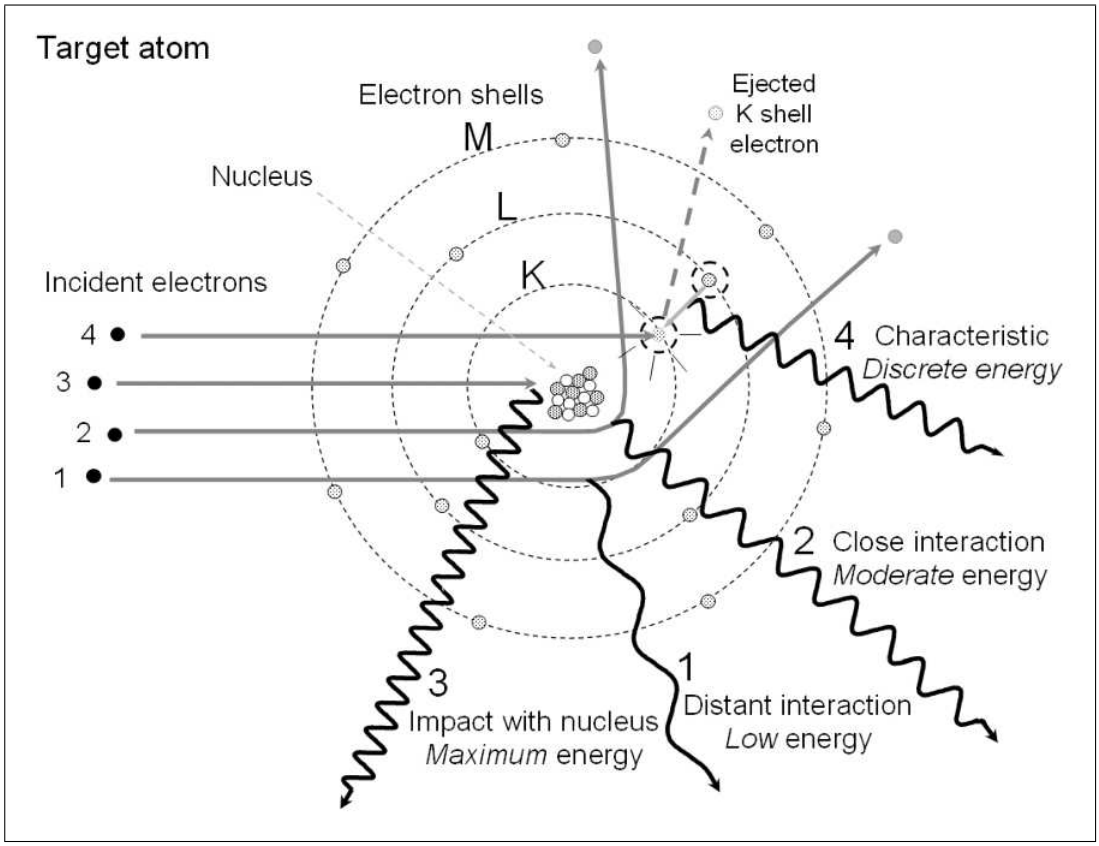


**Figure 2.1** The interactions of incident electrons with target atoms leading to x-ray photon emission.

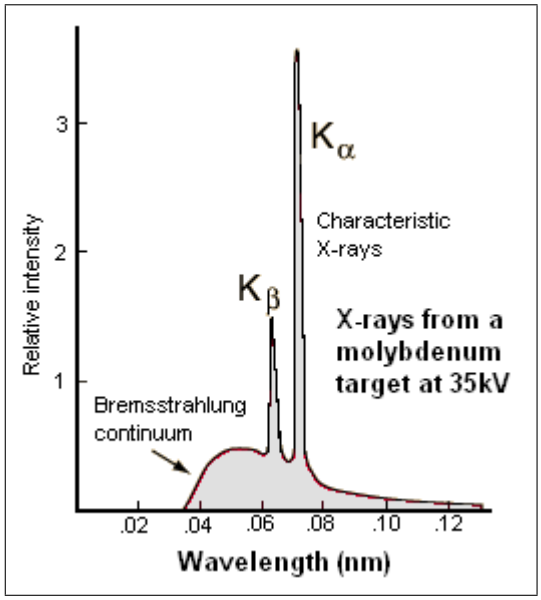


**Figure 2.2** The characteristic and Bremsstrahlung parts of the spectrum of a molybdenum target. [2]

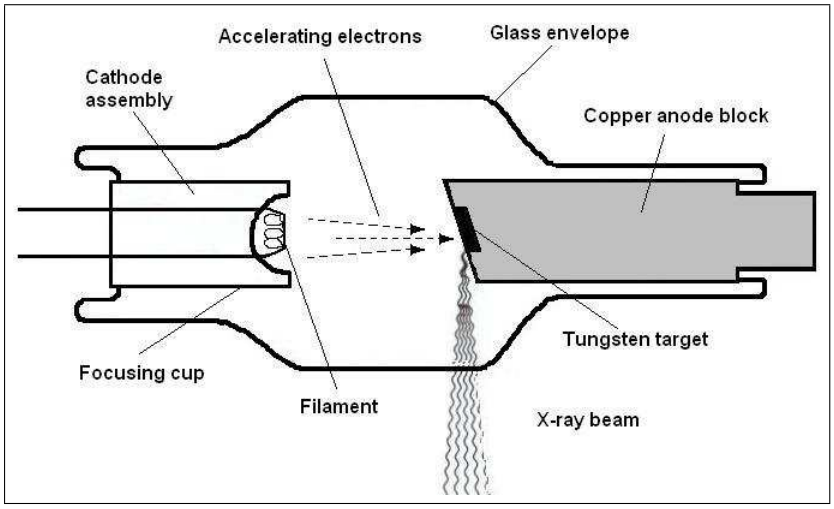


**Figure 2.3** The basic diagram of the X-ray tubes used in diagnostic X-ray machines. [3]

production, and its high melting point to endure high temperatures. Molybdenum is used as target material in mammographic X-ray tubes again due to its high melting point. A more important reason for using molybdenum is that its characteristic X-rays' energies (17.4 and 19.6keV) fall into the output spectrum when operating in the mammographic kV-range (25-28kV). As these electrons hit the target, X-ray photons are emitted as explained before and directed to the collimator and patient table. A rotating anode is used to distribute the heat to a circular region on the anode instead focusing on a small area which would cause damage due to high temperature generated during exposure. This lengthens the life of an X-ray tube.

To sum up, X-ray production typically involves bombarding a metal target in an X-ray tube with high speed electrons which have been accelerated by tens of kilovolts of potential. The bombarding electrons can either eject electrons from the inner shells of the atoms of the metal target or be decelerated by the nuclei of the metal atoms and generate X-ray photons [2]. The peak potential in the kilovolts range is the quantity to be measured.

## 2.2 Attenuation of X-rays in Matter

When the X-ray photons impinge upon a material they may either be absorbed (i.e. transfer their energy to the target atoms) or scattered or they may traverse the medium without interaction. Scattering and absorption events are related to attenuation of the whole X-ray beam in the material [12].

The number of photons attenuated in a medium depends on the number of photons transversing the medium. If the incident beam has 1000 photons and 20 of them are lost in the first unit thickness, only 980 enter the next one. Then out of 980 not 20 but proportionally 19 will be eliminated. There exists an exponential relationship between the intensities of the beam, before and after passing through a material of thickness $t$:

$$I = I_0 \cdot e^{-\mu \cdot t} \tag{2.1}$$

This important relationship is known as the Lambert-Beer Law, or the *Law of Exponential Attenuation.* [3] $\mu$ (in $\mathrm{cm}^{-1}$ or $\mathrm{mm}^{-1}$) in this equation is the linear attenuation coefficient. $e^{-\mu \cdot t}$ is the probability that a photon traverses the material of thickness $t$ without interacting. This probability is the product of probabilities that the photon does not interact by any of five interaction processes:

$$e^{-\mu t} = e^{-\omega t} e^{-\tau t} e^{-\sigma t} e^{-\kappa t} e^{-\pi t} = e^{-(\omega+\tau+\delta+\kappa+\pi)t}$$

The coefficients $\omega$, $\tau$, $\sigma$, $\kappa$, $\pi$ represent the attenuation by the processes of *coherent scattering* ($\omega$), *photoelectric absorption* ($\tau$), *Compton scattering* ($\sigma$), *pair production* ($\kappa$) and *photodisintegration* ($\pi$). Then, the total linear attenuation coefficient can be written as:

$$\mu = \omega + \tau + \sigma + \kappa + \pi \tag{2.2}$$

In diagnostic radiography, coherent scattering, photodisintegration and pair production

are usually negligible and $\mu$ reduces to:

$$\mu = \tau + \sigma \tag{2.3}$$

To measure $\mu$, two photodetectors with copper filters of different thicknesses are used as shown in Figure 1.1. The intensities of incident beams to the photodetectors are respectively:

$$I_1 = I_0 \cdot e^{-\mu \cdot t_1} \tag{2.4}$$

and

$$I_2 = I_0 \cdot e^{-\mu \cdot t_2} \tag{2.5}$$

The thicknesses $t_1$ and $t_2$ here are known. The intensities $I_1$ and $I_2$ are measured by the photodetectors. By taking their ratio $I_0$ is eliminated and the equation is solved for $\mu$:

$$ln\frac{I_1}{I_2} = \mu \cdot (t_2 - t_1) \tag{2.6}$$

and

$$\mu = \frac{ln\frac{I_1}{I_2}}{t_2 - t_1} \tag{2.7}$$

# 3. DESIGN PRINCIPLES

In this design, similarly to the commercial kVp-meters, the ratio of the intensities of the X-ray beam passing through different thicknesses of copper is used as the indicator of the kVp-level. The corresponding kVp value is obtained from a look-up table stored in the flash memory of a microcontroller. The exposure time is also measured by running an internal timer.

## 3.1 Device Block Diagram

Figure 3.1 shows the block diagram of the device. As the exposure starts the *photodetector* triggers the *timer* and start of the measurements. The X-ray beam incident to the *photodiodes* is filtered by different *Cu filters* and hence different currents are generated. These currents are fed into the *log-ratio amplifier*. The output is proportional to the logarithm of their ratio and is fed into an *Analog-to-Digital Converter* (ADC). The ADC and timer continue to run until the next signal from the trigger as the exposure stops. Then the measurement data is evaluated by the *microcontroller* and a corresponding kVp value is calculated using the *look-up table*.

Each block is explained in detail in the next sections.

### 3.1.1 Photodiodes

In the design Si photodiodes coupled to CsI scintillator with a very high X-ray sensitivity are used. The photodiodes (S8559, Hamamatsu Photonics Co., Hamamatsu, Japan) generate a current of 52nA for an exposure of 120kV, at 1mA tube current, 6mm Al filtration and at a distance of 83cm. These conditions, except the kVp and filtration are quite extreme conditions for detection. An X-ray machine usually operates at a minimum tube current of 100mA. The next stage log-ratio amplifier's dynamic range is

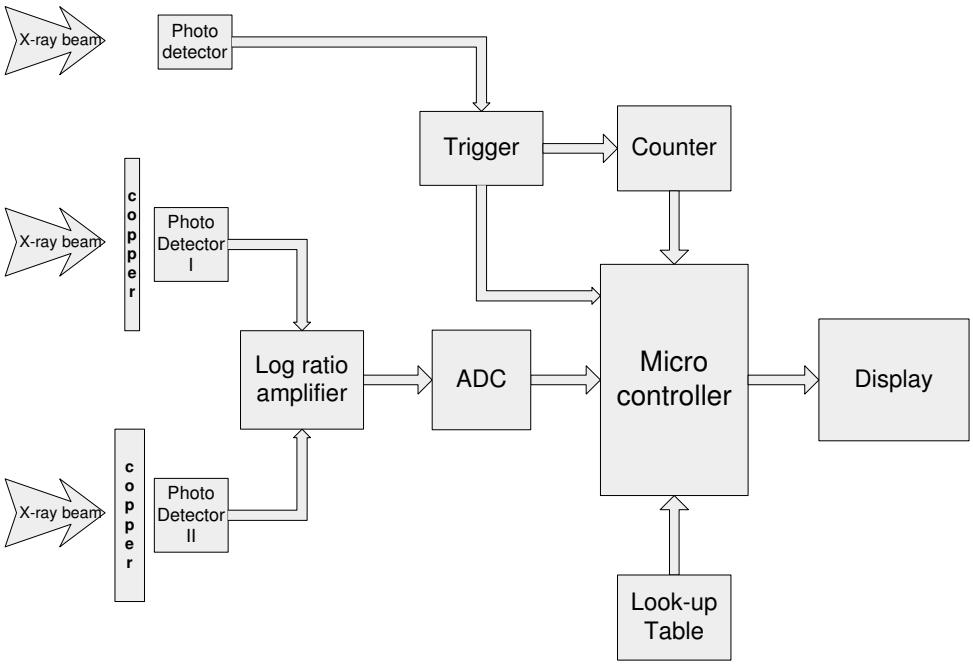


**Figure 3.1** Block diagram of the device

from 150pA up to 3.5mA. That is, the output will be linear for input currents down to 150pA, which is much less than the current expected to be generated during exposure. Taking into account the fact that the tube current is at least 100 times the reference value, it is certain that the current fed into the log-ratio amplifier will be sufficient.

One end of the photodiodes is connected to ground. Since the inputs of the log-ratio amplifier are also at ground potential due to its design, the photodiodes are at zero-bias and generate currents from cathode to anode when exposed to X-ray. (Figure 3.2) Therefore, in order to feed positive current, the cathode and anode pins are connected to ground and the input of the log-ratio amplifier, respectively.

### 3.1.2 Log-ratio Amplifier

As mentioned in the theory section, kVp is a function of the logarithm of the ratio of the two intensities. Therefore, a logarithm operation is required. Most digital kVp-meters do not compute the logarithm of the ratio, because logarithm computation

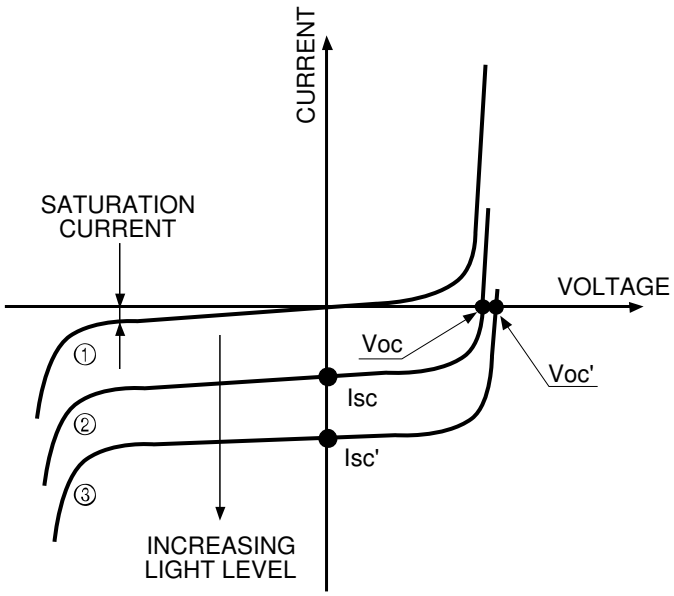


**Figure 3.2** Bias voltage-current characteristics

is very inefficient and slow. Instead, they only compute the ratio of the intensities using a microprocessor, but that is a slow operation, too. Additionally, using only the ratio information to find the kVp, would require 32-bit or higher resolution, which would further increase the computational burden and the look-up table would occupy too much space.

The logarithmic amplifier gives an analog voltage output proportional to the logarithm of the ratio of the input currents and without any time loss. The advantage of this log-ratio amplifier is that it reduces the computational burden on the microprocessor and therefore increases the speed of measurements.

A typical log-ratio amplifier consisting of two op-amps (A1 and A2) and a matched BJT-pair (Q1 and Q2) is drawn in Figure 3.3. Considering the relation between collector current $I_C$ and base-emitter voltage $V_{BE}$:

$$I_C = I_S \cdot e^{(V_{BE}/V_T)} \tag{3.1}$$

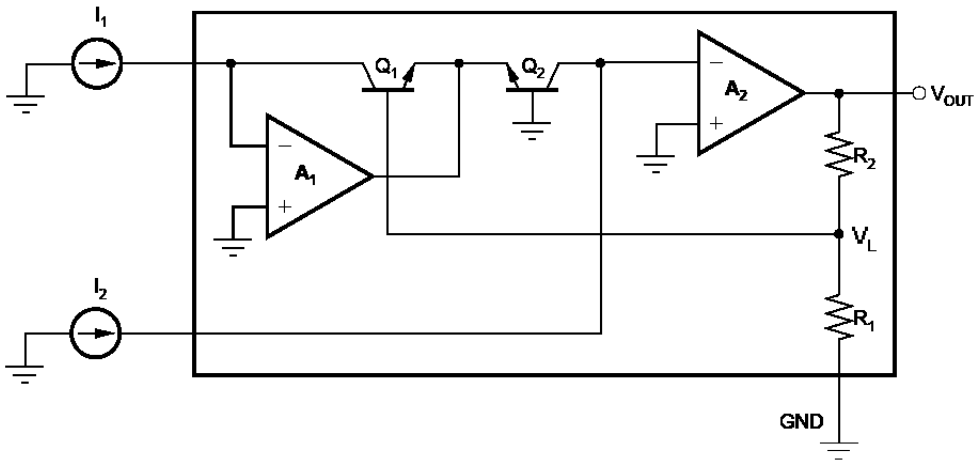


**Figure 3.3** Log-ratio amplifier. [4]

which leads to:

$$V_{BE} = V_T \cdot ln\frac{I_C}{I_S}$$

$V_T$ is thermal voltage at that temperature and $I_S$ is the reverse saturation current of BJT. In this circuit,

$$\begin{aligned} V_L &= V_{BE2} - V_{BE1} \\ &= V_T \cdot ln\left(\frac{I_{C2}}{I_{C1}} \cdot \frac{I_{S1}}{I_{S2}}\right) \end{aligned}$$

For matched BJT's the reverse saturation currents are equal and the collector currents are the input currents $I_1$ and $I_2$. So, the equation reduces to:

$$V_L = V_T \cdot ln\frac{I_2}{I_1}$$

Then,

$$V_{OUT} = \frac{(R_1 + R_2)}{R_1} \cdot V_L = \frac{(R_1 + R_2)}{R_1} \cdot V_T \cdot ln\frac{I_2}{I_1}$$

This equation shows that the output voltage is proportional to the logarithm of the ratio of the input currents. The logarithmic operation is solved by this circuitry and the computational burden on the microprocessor reduced significantly.

The LOG101 (Texas Instruments, Dallas, USA) IC gives a voltage output equal to the logarithm of the ratio of input currents ($I_1$ and $I_2$) to the base 10.

$$V_{OUT} = 1\text{V} \cdot log_{10}\frac{I_1}{I_2}$$

According to the data sheet this IC can operate from 150pA to 3.5mA input currents and can produce a maximum output of 3.5V when supplied from $\pm$5V. This corresponds to a maximum ratio of $10^{3.5} \cong 3162$. In this design, the thickness difference in filtering is 0.5mm Cu and the linear attenuation coefficient for copper does not exceed $15\text{mm}^{-1}$ down to 25keV [1]. The ratio of the intensities at 25keV is then,

$$e^{0.5mm \cdot 15mm^{-1}} \cong 1808$$

So, by remembering that the effective energy spectrum of an X-ray tube never goes below this level, LOG101 can be safely used.

Since the number of distinct kVp levels depends on the resolution of the ADC, a 10-bit ADC is sufficient.

### 3.1.3 Trigger

The triggering function is very simple: it will detect the start of exposure and wake-up the microcontroller. It consists of a non-X-ray cheap photodetector (OPT101, Burr-Brown Products of Texas Instruments, Dallas, USA) with a large feedback resistance, a single analog comparator and a reference voltage connected to the negative input of the comparator. The output of the photodetector is connected to the positive input of the comparator. When the photodetector voltage exceeds the reference voltage, the trigger's output switches from 0 to logic 1 and triggers the microcontroller. In fact, the microcontroller ATmega16 used in this project has an analog comparator built in it and no additional IC is needed. As threshold, a voltage as small as 50mV is selected, because the photodetector is not sensitive to X-ray and the output voltage generated during exposure is small. In addition to the internal 1MΩ an additional 56MΩ feedback resistance is connected to increase the gain.

### 3.1.4 Analog-to-Digital Converter

As discussed above, the number of kVp levels that are resolved directly depends directly on the resolution of ADC. In the beginning, it is almost impossible to guess how many bits of voltage information are required to resolve the kVp in steps of 0.1kV. The microcontroller ATmega16 also has a 10-bit ADC built in, which can represent the voltage information in $2^{10} = 1024$ levels. By using this ADC it is also possible to save one IC on the board.

The important point here is whether the speed of this ADC is sufficient to sample the waveform. In the data sheet of ATmega16 the maximum frequency to run the ADC for 10-bit resolution is given as 200kHz. Running the ADC at frequencies higher than this would result in incorrect results. The ADC circuitry needs 13 clock cycles for one conversion if running in auto triggered mode. This mode can be selected at programming. Dividing 200kHz by 13 cycles per conversion results in 15.4 kS/s. However, for an even better signal-to-noise ratio (SNR) averaging can be considered.

Averaging with 8 consecutive samples decreases the sampling frequency to:

$$15.4 \text{ kS/s}/8 \cong 1.9 \text{ kS/s}$$

Most X-ray machines are operating at very high frequencies and have an output with very low ripple and consequently very close to DC. To sample these waveforms 1.9 kS/s is more than adequate. But, there are still around some X-ray machines operating at single phase or even self rectified. The problem here is whether this sampling frequency is sufficient not to miss the peaks of the wave. To test this accurately, the worst case should be considered, where the maximum point is missed by a half cycle of the sampling frequency of ADC. In this case, the peak at 5ms is missed by 32.5$\mu$s. Then, the time points to sample a 50Hz sine wave and the corresponding results are given in Table 3.1.

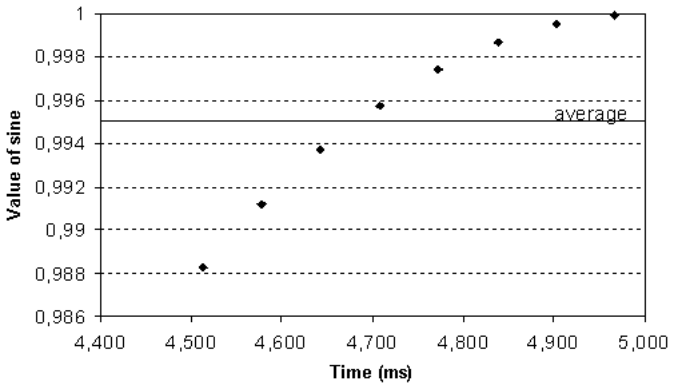


**Figure 3.4** Approximation to sine wave

As seen from Figure 3.4 and Table 3.1, the error is about 0.5%, and can be neglected. Averaging over 8 consecutive samples is not disturbing the measurement result and makes the system more immune to noise or random fluctuations in the intensity of the incident beam which are independent of kVp level. As reference voltage for the ADC, the internal 2.56V of the microcontroller is used instead of an external voltage, since the power supply voltage can change due to loading effect which would lead to inaccurate conversions. The $V_{REF}$ pin of the microcontroller is by-passed with a 10nF capacitor and the input of the power supply pin of the ADC ($A_{VCC}$) is filtered

**Table 3.1**
Approximation to sine wave

| Sampling instant (ms) | Value of sine |
|---|---|
| 4.968 | 0.99994788 |
| 4.903 | 0.99953095 |
| 4.838 | 0.99869725 |
| 4.773 | 0.99744715 |
| 4.708 | 0.99578115 |
| 4.643 | 0.99369996 |
| 4.578 | 0.99120443 |
| 4.513 | 0.98829562 |
| Average: | 0.99557555 |

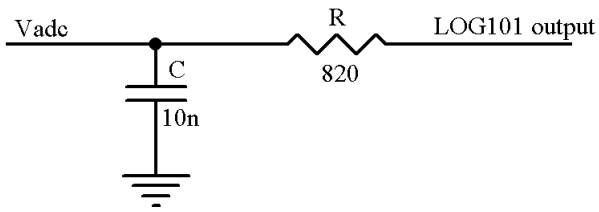


**Figure 3.5** 20kHz low-pass filter at the input of the ADC.

by an LC network as recommended in the data sheet. The inductor and capacitor values are 10$\mu$H and 100nF, respectively.

To further immunize the measurement results to 350kHz noise which is caused by the switching nature of the negative power supply IC, as explained later in section 3.4.2, a 1$^{st}$ order filter is placed before the input of the ADC. This is an RC filter with R = 820$\Omega$ and C = 100nF such that $f = \frac{1}{2\pi \cdot RC} \cong 20$ kHz (Figure 3.5).

### 3.1.5 Microcontroller

The microcontroller unit ATmega16 (Atmel Co., San Jose, California, USA) is the leading component of the circuit. ATmega16 has a RISC architecture processor but the instruction set is as powerful as in a CISC architecture chip and this makes ATmega16 a very fast processor. For instance, multiplication is performed by a single instruction and over 2 cycles without long series of adding and shifting instructions otherwise. Other arguments for using this microcontroller are as follows:

- 10-bit ADC, to save one ADC-IC if 10-bit operation suffices. In addition to this, ATmega16 has also an internal reference voltage of 2.56V.
- Internal analog comparator, to save one comparator IC on the board.
- Timer, necessary to measure the exposure time.
- 16 Kbytes of flash program memory, suitable for C compiler usage. 16 Kbytes are so huge for this project, that coding the program in a C environment is possible without worrying about the size. A limited size of program memory would result in more care about the size of the code, even time consuming assembly coding would be necessary to deal with limited resources.
- 1 Kbytes of RAM. This amount of RAM makes storage of long arrays consisting of ADC results and operations on these numbers possible. Data on RAM is lost after the power is shut down.
- Serial Peripheral Interface (SPI). SPI is a very important feature for microcontrollers to be able to communicate with other microcontrollers and other components supporting this feature. As it is a bus, communication with many components is possible. For example, many ADC IC's support this feature and the voltage information is sent to the microcontroller through SPI. Even it is not used in this design, an unsoldered footprint for an ADC is available on the PCB and may be used in next versions.

- 3.8mA of current consumption in active mode at 4 MHz. Since the maximum frequency for the ADC is 200kHz and it is obtained by dividing the CPU frequency by the powers of 2, the best frequency of operation seems to be 3.2MHz, since it is 16th multiple of 200 kHz and 16 CPU clock cycles are enough to complete arithmetic and storage operations on 2 bytes (10-bit) data until the next data comes. 3.8mA is quite low and taking the short operation durations (1-2 min per machine) into account, it can be inferred that the battery life will be quite long.

The microcontroller in this circuit becomes active as the power is switched on. At the start it initializes itself and waits for the trigger signal from the analog comparator. As the comparator switches to high, the microcontroller starts the ADC to measure the voltage from the log-ratio amplifier and starts the 16-bit internal timer to measure the exposure time. During exposure the trigger signal is always HIGH and the ADC repetitively samples the output of the log-ratio amplifier. After every eighth sampling, the average of the previous eight samples is computed and stored in an 24-element array in the RAM. As the array gets full after the $24^{\text{th}}$ value is stored, the minimum of these 24 values is found which corresponds to the highest kV during the formation of this array and stored in another 24-element array of minimum values. As a matter of fact, the minimum value of this array corresponds to the highest kV during the whole exposure. Since both arrays have 24 elements and each value is obtained by averaging over 8 consecutive samples, it takes $24 \times 24 \times 8$ samples $= 4608$ samples until all these arrays are full. With the sampling frequency of 15.4kS/s, this corresponds to approx. 300ms. That is, the kVp for a long exposure is found from the measurements conducted in the first 300ms. However, the timer keeps counting until the trigger signal is cleared. The prescale value for generating the timer clock frequency from the CPU frequency is selected as 256. Therefore the timer clock frequency is 3.2MHz / 256 $\cong$ 12.77 kHz. For an overflow of the 16-bit timer running at this frequency $2^{16}$/12.77kHz $\cong$ 5s are needed. This means, that the device can measure exposure times up to 5s and with a resolution of 1/12.77kHz $\cong$ 0.1ms. The accuracy depends on the crystal used and is usually less than 100 ppm.

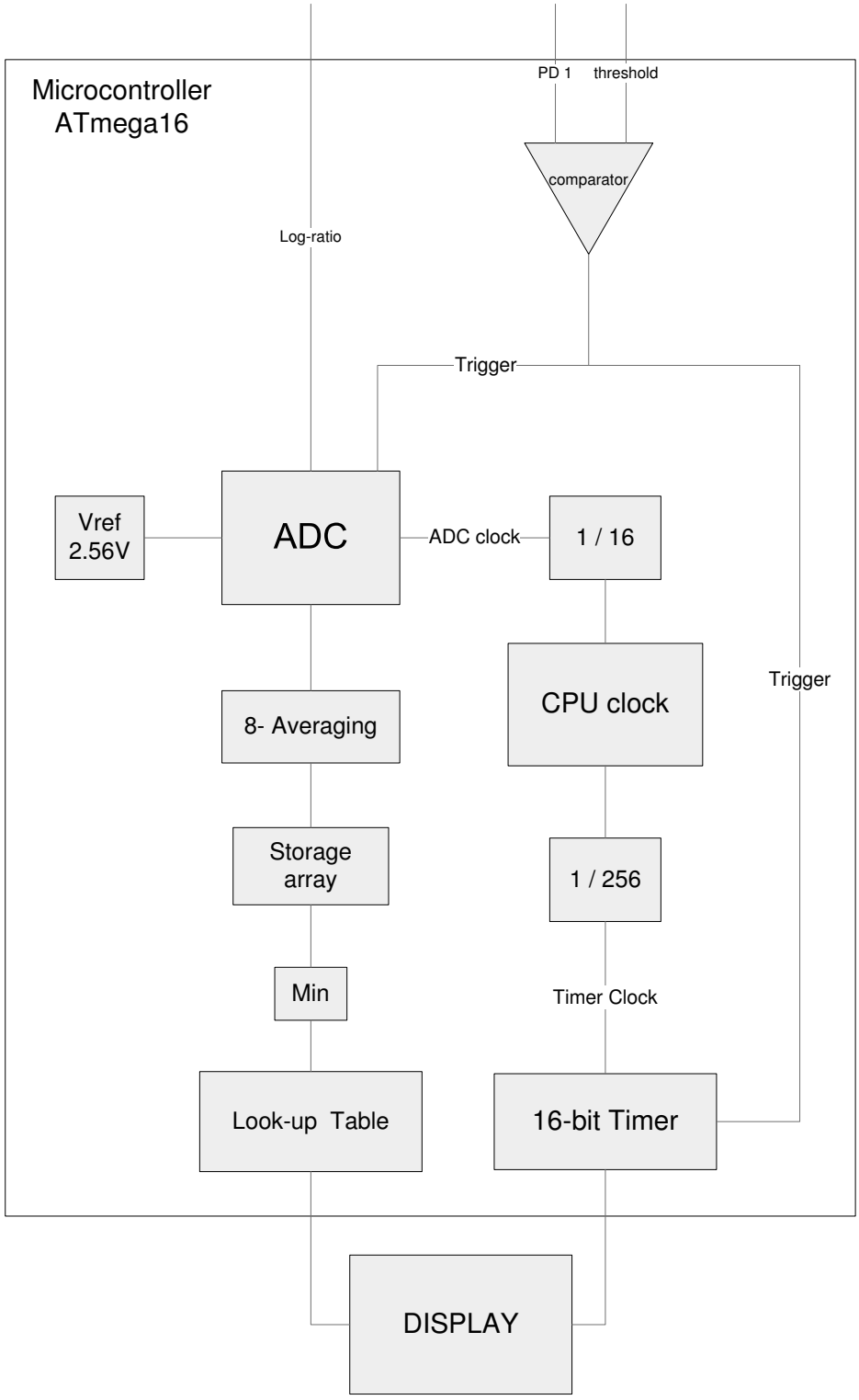


**Figure 3.6** Block diagram of the microcontroller

The code running the microcontroller will be discussed in the section 3.2.

### 3.1.6 Look-up Table

The look-up table contains the reference values for the measurements. The microcontroller finds for each measurement a corresponding kVp value from the look-up table by linearly interpolating between the reference values.

The look-up table is directly related to the accuracy. The more correct the numbers in the look-up table are, the more accurate the measurements will be. The most important point in creating a look-up table is that the spacing of the reference values does not cause errors larger than 0.1kVp, because linear interpolation is utilized. The formation of the first look-up table is another important point. The next ones will be then just small adjustments on the first one. The spacing of the reference values and formation of the first look-up table will be discussed in section 3.3.

## 3.2 The Microcontroller Code

The flow chart of the microcontroller code is shown in Figure 3.7.

### 3.2.1 Initialization

**3.2.1.1 Ports.** The first block is initialization. During initialization, the levels of the four ports, namely PORTA, PORTB, PORTC, PORTD are all reset to logic 0 or 0V and their data direction registers DDRA, DDRB, DDRC, DDRD are set according to the connection type of each pin. As seen in the Figure 3.8, the connections of the pins are as follows: PORTA is the ADC port of ATmega16. All the 8 pins can be connected to an analog voltage input. However, in this design only one pin is used. PORTA 0-6: Not connected. To avoid noise, these pins are set as outputs and to logic

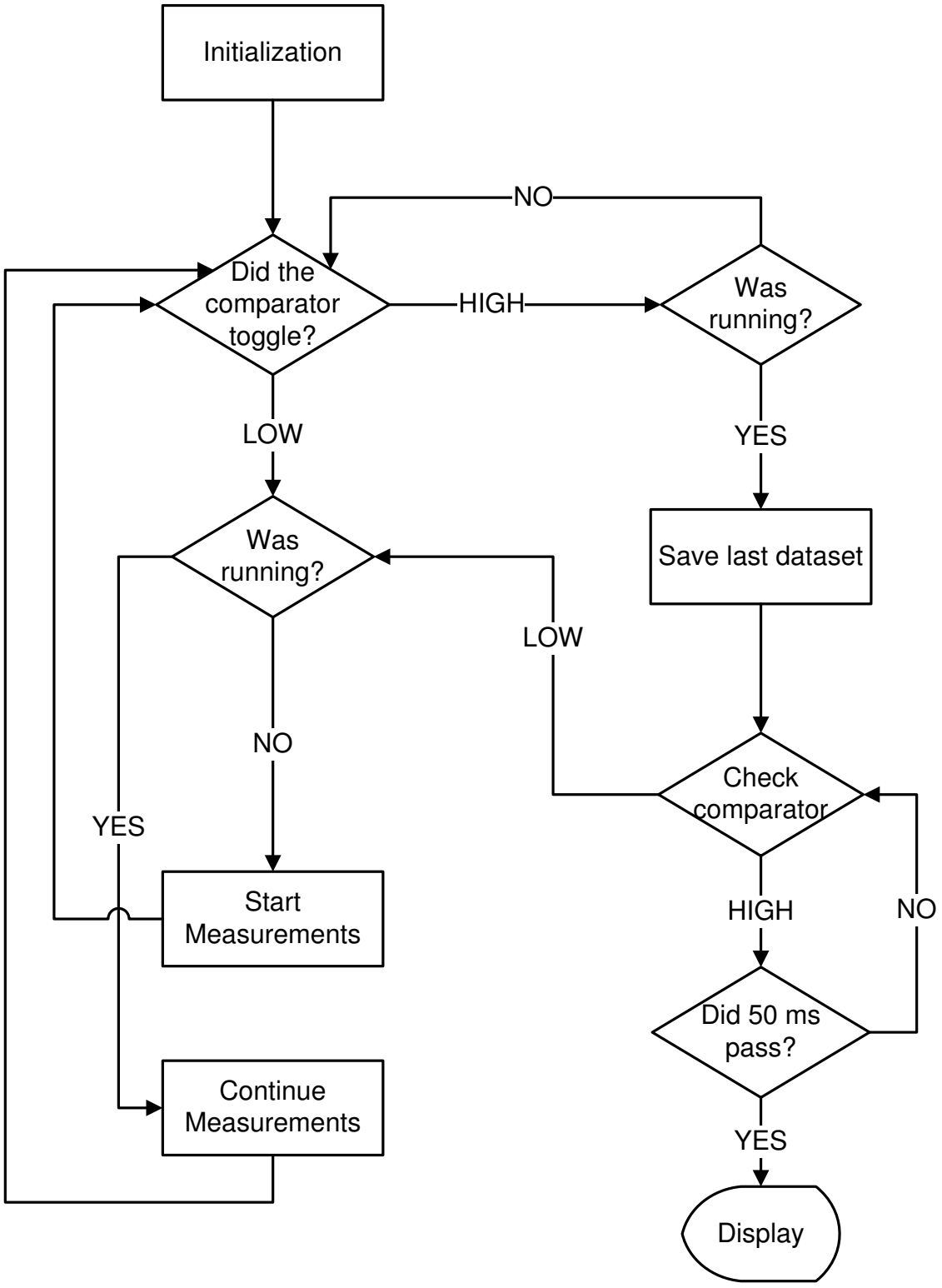


**Figure 3.7** Flow chart of the microcontroller code

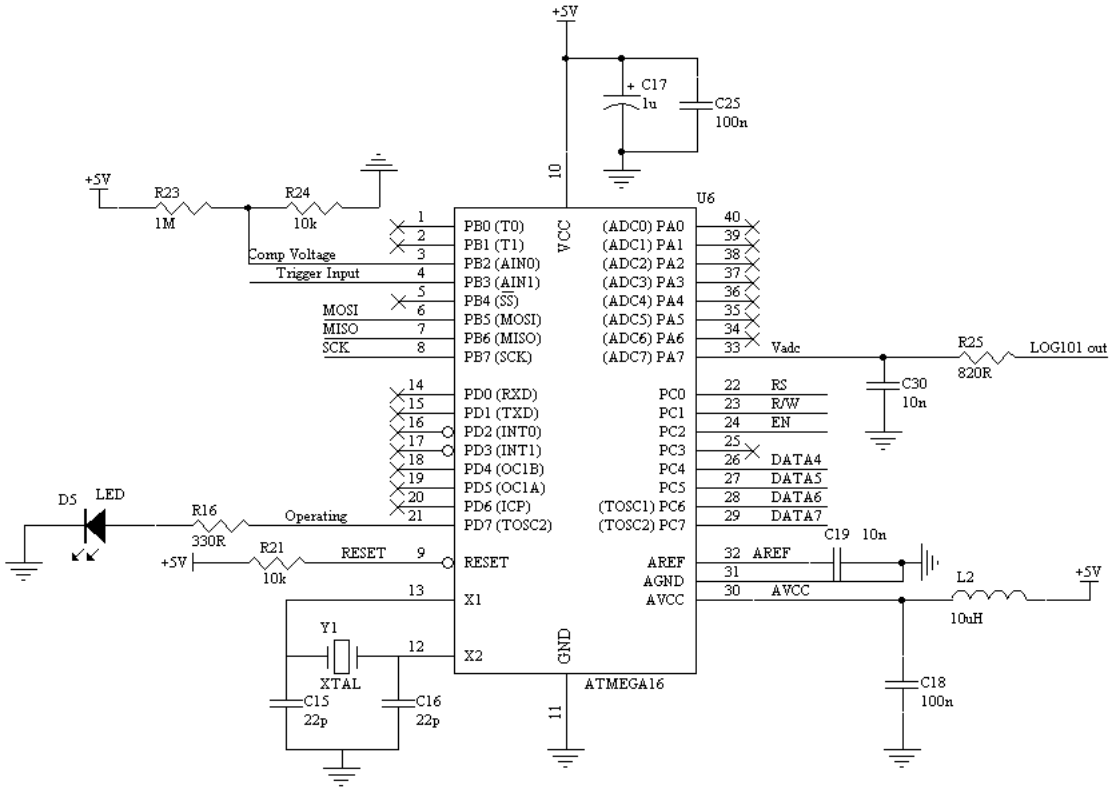


**Figure 3.8** The connections of the micrcontroller ATmega16

0. PORTA 7: This is the ADC pin and therefore it is an input.

So, the register PORTA is set to 0000 0000 and the DDRA is set to 0111 1111.

PORTB 0-1: Not connected. To avoid noise, these pins are set as outputs and to logic 0.

PORTB 2-3: Inputs of the internal analog comparator. So, they are set as inputs.

PORTB 4-7: Pins of SPI. Since there is no device connected to the SPI bus, they are not used and set to logic 0.

So, the register PORTB is set to 0000 0000 and the DDRB is set to 1011 0011.

PORTC is set as the LCD display interface of ATmega16.

PORTC 0: RS (Register Select) This pin is pulled to HIGH or LOW, to select one of the internal registers of the LCD. Therefore it is an output and is initially set to logic 0.

PORTC 1: R/W (Read / Write) This pin is connected to the R/W input of the LCD and selects the mode of operation and all the time the mode of operation is WRITE mode. Therefore, this pin is an output and set to logic 0.

PORTC 2: EN (ENable) This pin is connected to EN input of the LCD and enables it if written logic 0. Therefore it is an output and set to logic 0.
PORTC 3: Not connected. To avoid noise, this pin is set as output and to logic 0.
PORTC 4-7: The parallel data lines from the microcontroller to the LCD. Therefore these pins are outputs and initially set to logic 0.

So, the register PORTC is set to 0000 0000 and DDRC is set to 1111 1111. PORTD is used mainly as digital outputs or inputs to make the user to be able to select any mode of operation and drives LEDs to inform. In this design however, there is only one mode of operation, namely the roentgen mode. Therefore, the user is not able to change it. If new features are added in the future, these pins can be used either as digital inputs or outputs. The only pin used drives a LED to indicate exposure.
PORTD 0-6: Not used. To avoid noise, this pin is set as output and to logic 0.
PORTD 7: This pin drives a LED during exposure and is a mark of proper operation of the device. This pin is initially set to logic 0 and reaches 5V if set to logic 1 during operation. The LEDs have usually a voltage drop of 1.8V. The maximum current allowed from a single pin is given as 40mA. To limit the current through the LED to 10mA, which is quite safe, a 330Ω resistor is put in series with the LED. So, the register PORTC is set to 0000 0000 and DDRC is set to 1111 1111. A summary of the Data Direction Registers and the initial settings of the ports is in Table 3.2

**Table 3.2**
The initial settings of the ports.

| PORT | A | B | C | D |
|---|---|---|---|---|
| Output | 0000 0000 | 0000 0000 | 0000 0000 | 0000 0000 |
| DDR | 0111 1111 | 1011 0011 | 1111 1111 | 1111 1111 |

**3.2.1.2 Analog to digital converter.** The ADC is initialized by setting the ADMUX, ADCSRA and SFIOR registers (Table 3.3).

The first 5 bits of ADMUX are used to set the input source. In this design

the $7_{th}$ pin is selected as the ADC input. Therefore a binary 7 is written to these bits. Since the ADC can give 10-bit results there can be distinguished two modes of result. ADLAR should be set if a left adjusted conversion is desired. In this design, all the 10-bits are required and this bit is kept as logic 0. REFS0 and REFS1 bits are used to select the reference source. Since the internal 2.56V reference is used in this design, these bits are set to 11 regarding the data sheet. At the end, ADMUX is set to 11000111.

At initialization the ADC is turned off. ADEN, ADSC, ADATE, ADIF, ADIE of ADCSRA are reset. To select the prescaler of the ADC clock as 16, 100 is written to the ADPS bits. At the end, ADCSRA is set to 00000100. This ADC will be run in

**Table 3.3**
The ADC registers after initialization

| Bits | 7 | 6 | 5 | 4 | 3 | 2 | 1 | 0 |
|---|---|---|---|---|---|---|---|---|
| ADMUX | REFS1 | REFS0 | ADLAR | MUX4 | MUX3 | MUX2 | MUX1 | MUX0 |
| Value set | 1 | 1 | 0 | 0 | 0 | 1 | 1 | 1 |
| ADCSRA | ADEN | ADSC | ADATE | ADIF | ADIE | ADPS2 | ADPS1 | ADPS0 |
| Value set | 0 | 0 | 0 | 0 | 0 | 1 | 0 | 0 |
| SFIOR | ADTS2 | ADTS1 | ADTS0 | - | - | - | - | - |
| Value set | 0 | 0 | 0 | - | - | - | - | - |

"free running" mode. Namely, each conversion should trigger the following conversion. This feature is selected by setting the $7^{th}$, $6^{th}$ and $5^{th}$ bits of SFIOR register. The other bits of this register are not related to ADC.

**3.2.1.3 Analog comparator.** The analog comparator provides the trigger signal for the microcontroller to start conversions. Therefore it is switched on at the start and set to interrupt every time the output toggles. To enable the analog comparator the ACD (analog comparator disable) bit is reset, to enable the analog comparator interrupt, the ACIE (analog comparator interrupt enable) bit of the ACSR (Comparator control and Status Register) is set. To select the interrupt on toggle mode the ACIS1

**Table 3.4**
The ACSR register to initialize the analog comparator

| Bits | 7 | 6 | 5 | 4 | 3 | 2 | 1 | 0 |
|---|---|---|---|---|---|---|---|---|
| ACSR | ACD | ACBG | ACO | ACI | ACIE | ACIC | ACIS1 | ACIS0 |
| Value set | 0 | 0 | 0 | 0 | 1 | 0 | 0 | 0 |
| SFIOR | - | - | - | - | ACME | - | - | - |
| Value set | - | - | - | - | 0 | - | - | - |

and ACIS0 bits are reset. After initialization ACSR is 0000 1000. The remaining bits are outputs of the analog comparator. Since no input multiplexing is needed, ACME in the SFIOR is reset.

**3.2.1.4 LCD display.** The initialization of the LCD display is done easily by using the embedded *lcd_ init()* function of the CodeVision C compiler. This function accepts only the number of columns as parameter. Therefore it is used in the form lcd_init(16) in the source code.

**3.2.1.5 Timers and external interrupts.** The timers are all stopped during initialization. The timer will be run only after an interrupt occurs. All the timer registers are reset. All external interrupts are disabled, since none is used. The corresponding registers in the microcontroller are all reset.

The last and most important step is to set the global interrupts. To set the global interrupts the assembly command "**sei**" is used. Without setting the global interrupts, the analog comparator cannot provide an interrupt and the device cannot start. But this is done as the last step to avoid any undesired results. The summary of initialization is given in Figure 3.9 The connections to other pins are explained below.
**RESET**: If this pin is pulled down to logic 0 a reset condition occurs, which should be avoided in this design. Therefore this pin is pulled up using a 10k resistor.
**X1** and **X2** are the pins where the 3.2MHz crystal is connected with small capacitances

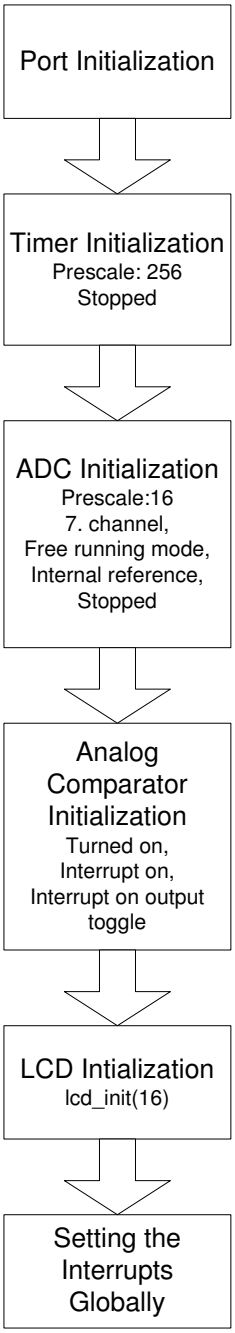


**Figure 3.9** Initialization

to ground as recommended in the data sheet.

$\mathbf{V_{CC}}$ is the power supply of the microcontroller. It is by-passed with a $1\mu$ F and 10nF ceramic capacitors to ground to avoid large fluctuations in power supply voltage.

$\mathbf{A_{VCC}}$ is the separate power supply of the ADC and should be provided a very smooth 5V. As recommended in the data sheet an LC network of $10\mu$H and 100nF filters the power supply voltage.

$\mathbf{A_{GND}}$ is the ground of the ADC. It should be provided a separate ground line from the main power supply to this pin.

$\mathbf{A_{REF}}$ is connected to the reference voltage of the ADC. Since the internal reference is used in this design, it is by-passed with a 10nF capacitor to ground as recommended in the data sheet.

### 3.2.2 Operation

After initialization the microcontroller enters an infinite while loop and waits for an interrupt from the analog comparator to break. If the output of the comparator toggles it first checks whether the output is at LOW or at HIGH state. A LOW means the photodetector output is greater than the 50mV reference voltage and corresponds to an exposure. Once waken up, the microcontroller checks whether the device was running before by testing the flag *running*. If *running* is 1, it means that the device was running. Otherwise the microcontroller starts the analog to digital conversions and the 16-bit timer and sets *running* to 1. To start the ADC and to enable the auto-trigger mode, logic 1 is written to ADEN and ADATE bits of the ADCSRA (Table 3.3).

The next interrupt will occur when the photodetector voltage drops below the reference voltage and the comparator output switches from LOW to HIGH. This does not necessarily mean the end of the exposure. In single phase X-ray machines, the output spectrum changes with the sinusoidal varying kV and as the kV drops below a certain level there may be no higher energy X-ray photons emitted and the signal drops. If the next interrupt occurs, the microcontroller first waits for the current conversion to complete and shuts the ADC down, where the timer keeps counting. To

check whether this drop was due to single phase sinusoidal changing kV or the exposure was really over, it waits for 50ms. 50ms is selected because it is longer than the 20ms period of 50Hz. In this 50ms, if a new interrupt occurs, namely the comparator toggles from HIGH to LOW, the microcontroller starts the conversions again and continues collecting data, because the flag *running* is 1. If no interrupt occurs, this means, that this is really the end of the exposure. Then, the microcontroller, stops the timer, resets *running*, finds the minimum value among the data and computes the corresponding kVp value from the look-up table. The exact duration of the exposure is the time recorded by the timer minus 50ms. Then it computes the exposure time and displays the results. Now, it is ready for the next exposure. The data is not saved and the results of the next exposure overwrite those of the previous exposure.

## 3.3 Generation of the Look-up Table

To form the first look-up table, an accurate X-ray machine (Siemens Multix Compact K, Siemens AG, Erlangen, Germany), a recently calibrated dosimeter (Radcal 2026C, Radcal, Monrovia, CA, USA) and various metal filters of different thicknesses (2mm Al, 0.5mm Cu, 1mm Cu) are used. The procedure is described below:

First of all, 2mm is the thickness of the aluminum filter which is used to absorb the low energy photons and shift the effective kV to right, namely to harden the beam. Thicknesses larger than 2mm may cause problems when using with low mA, i.e. less powerful machines. The X-ray intensities produced by these machines may not be strong enough to induce a current after being filtered by a thick aluminum layer and 1mm copper. The procedure is to measure the dose using the 0.5mm and 1mm Cu filters. By putting the Al and Cu filters of different thicknesses in front of the ionization chamber, the doses measured at different kVp levels were recorded, while mAs and SID(source-to-image distance) were kept constant. The dose is directly proportional to the intensity. Therefore, dose is a valid measure for intensity and their ratios will be equal to the ratios of the intensities. Initial dose measurements at different kVp levels are given in Table 3.5 and plotted in Figure 3.10.

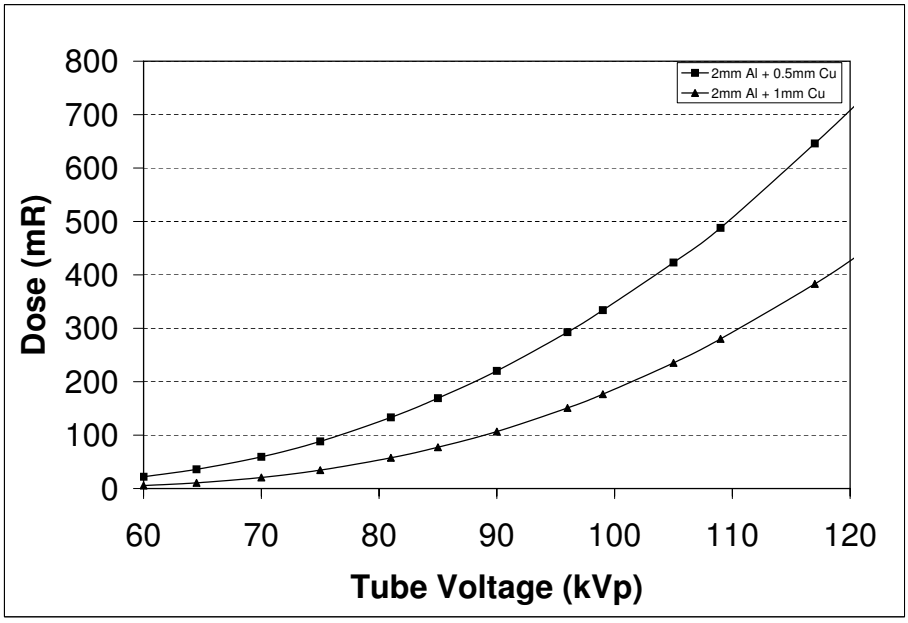


**Figure 3.10** Dose delivered vs. kVp for varying Cu thicknesses.

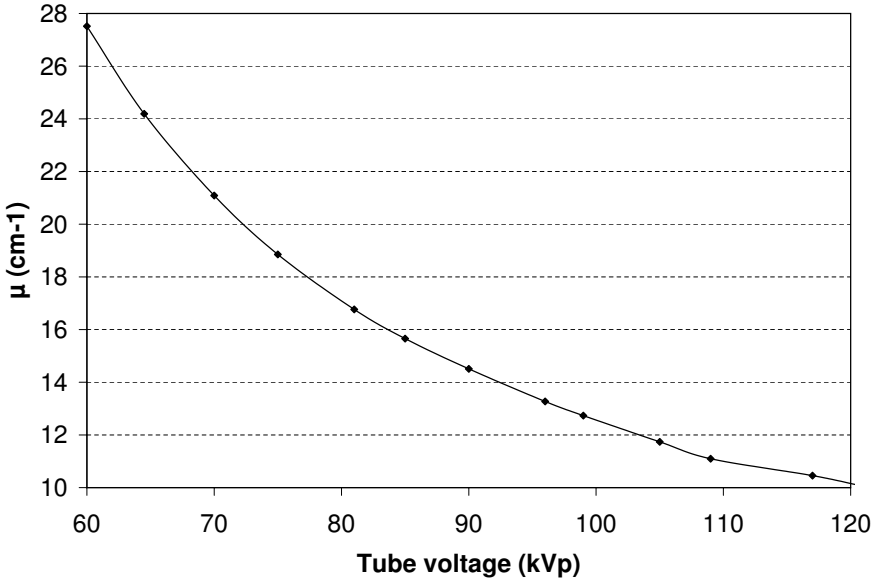


**Figure 3.11** Linear attenuation coefficient vs. kVp.

**Table 3.5**
Doses measured by using Cu filters of different thicknesses and the logarithms of their ratios

| kVp | Dose Level (mR) | | Ratio | Logarithm of ratios | |
|---|---|---|---|---|---|
| | 2mm Al + 0.5mm Cu | 2mm Al + 1mm Cu | | $ln$ | $log_{10}$ |
| 60 | 22.1 | 5.56 | 3.975 | 1.376 | 0.598 |
| 64.5 | 35.9 | 10.71 | 3.352 | 1.210 | 0.525 |
| 70 | 59.3 | 20.66 | 2.87 | 1.054 | 0.458 |
| 75 | 88.3 | 34.4 | 2.567 | 0.943 | 0.409 |
| 81 | 133.2 | 57.6 | 2.313 | 0.838 | 0.364 |
| 85 | 169.1 | 77.3 | 2.188 | 0.783 | 0.340 |
| 90 | 220.2 | 106.6 | 2.066 | 0.725 | 0.315 |
| 96 | 292.8 | 150.8 | 1.942 | 0.664 | 0.288 |
| 99 | 334 | 176.7 | 1.89 | 0.637 | 0.277 |
| 105 | 423 | 235.2 | 1.798 | 0.587 | 0.255 |
| 109 | 488 | 280.2 | 1.742 | 0.555 | 0.241 |
| 117 | 646 | 383 | 1.687 | 0.523 | 0.227 |
| 121 | 729 | 441 | 1.653 | 0.503 | 0.218 |

As seen from Figure 3.11, the linear attenuation coefficient of Cu varies between 2.6mm$^{-1}$ and 1mm$^{-1}$ in the diagnostic range 60-120kVp. However, $\mu$ for photons with energies 60-120keV is given as 12.5mm$^{-1}$ and 3mm$^{-1}$ [1]. This difference is caused by the fact that the beam does not contain only photons of the maximum energy but also and mostly of lower energies due to Bremsstrahlung and characteristic radiation.

Since the kVp is a function of the linear attenuation coefficient $\mu$, the necessary data to build up the look-up table is the logarithm of the ratios. However the log-ratio amplifier used in this design provides a voltage proportional to the logarithm of the ratio to the base 10. Namely, the voltage at the output of LOG101 is $log_{10}(I_1/I_2)$ rather than $ln(I_1/I_2)$.

It is assumed that the values in the $log_{10}$ column are also equal to the output of LOG101 in volts. Since the reference voltage of the ADC in ATmega16 is 2.56V and voltages up to this level can be fed to the input, it is necessary to further amplify the

output of LOG101 to increase the resolution. For this purpose, a non-inverting op-amp network with a DC gain of 4 is added, because the ADC accepts only positive inputs and also the op-amps (MAX4477, Maxim/Dallas, Sunnyvale CA, USA) used here are powered from +5V single supply. There is no possibility to obtain negative voltages.

Since the package of MAX4477 includes two op-amps, the other one is used to buffer the output of the first op-amp and drive a BNC output. This BNC output is used to track the signal generated by the log-ratio amplifier on an oscilloscope in the development stages. The reason to buffer the output is to minimize the load on the amplifier due to long BNC cables and avoid any noise caught by these cables connecting to another instrument.

To make the kVp computations easier, the reference values should be selected in equal increments. This is the logic behind look-up table. The values used in dose measurements do not form an equally spaced table. Using Matlab's curve fitting tool (The MathWorks Inc., Natick MA, USA) these values were fitted to a exponential function and the new values were calculated. The advantage of curve fitting is that the curve gets smoother any small discontinuity caused by measurement errors, disappears. Otherwise, it was also possible to calculate these values by linearly interpolating between the measurement data. Matlab found the following relation between kVp level and voltage at the input of the ADC:

$$V_{adc} = 52.71e^{-0.0659 \cdot kVp} + 2.024e^{-0.006279 \cdot kVp} \tag{3.2}$$

This look-up table was used in the first kVp measurement and then corrected according the results. As seen from Table 3.6, the values are spaced in 32-step intervals. The zeros are the kVp levels beyond the capability of the X-ray machines and used as an indicator of an error occurred during measurement.

To find the error caused by the linear interpolation between 32-step intervals, for each section the middle point is taken into account, because the maximum deviation from the true result will be in the middle point of the interval. The maximum errors

for each interval are shown in Table 3.6.

The first column of Table 3.6 shows the ADC outputs. The values in the second column are found from dose measurements and represent the first look-up table. The third column gives the corrected reference values. The next table shows the values found both by linear interpolation between the reference values and by the Equation 3.2, which represents the true result. The last column shows the error of the linear interpolation.

## 3.4 Power Supply

The components in this circuit with power connections are MAX4477, LOG101, ATmega16 and LCD display. All expect the LOG101 operate with a single +5V. LOG101 works with ±5V dual supply. So, this circuit will have two voltage sources. The main supply of power is a 9V battery. A low dropout voltage regulator (MAX883, Maxim/Dallas, Sunnyvale CA, USA) is used to obtain a smooth +5V to drive the IC's. MAX883 can supply current up to 200mA with only 220mV dropout. The negative voltage is obtained using a DC-DC inverter (MAX1673, Maxim/Dallas). The +5V obtained from the regulator is fed as reference and this IC produces a negative voltage equal to it.

### 3.4.1 +5V Power Supply

The Figure 3.12 shows the schematics of the positive power supply. The battery is connected to the input of the MAX883 through a diode, to prevent any damage that may occur when the polarities are reversed. The large 10$\mu$F by-pass capacitor ensures a smoother input voltage when the battery cannot supply enough current under sudden loading condition. The MAX883 has an adjustable output but in this design the preset output 5V is used and therefore the SET pin is connected to ground as described in the data sheet. The MAX883 has also a low-battery indicator. If the

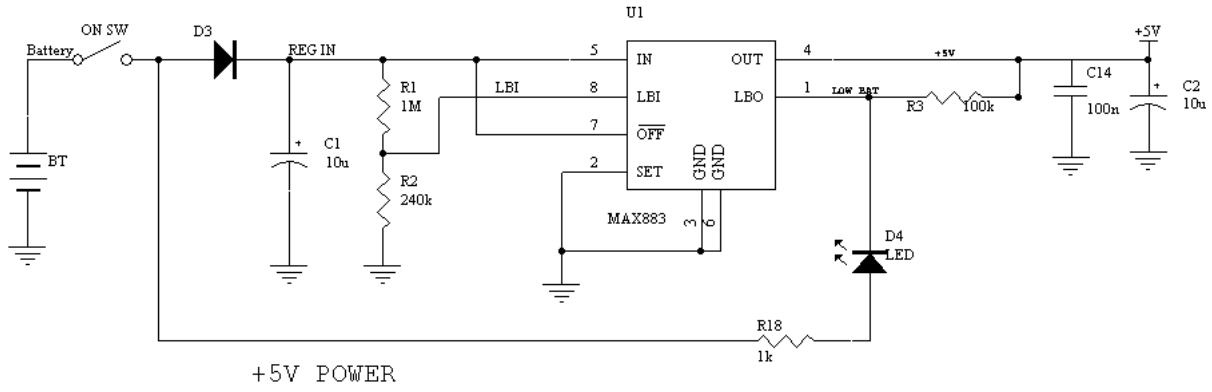


**Figure 3.12** +5V regulated power supply

voltage at the LBI pin drops below 1.2V the open drain output at LBO pin goes down to ground and the LED turns on. Otherwise the open drain prevents any current flow through the LED and it remains off. With the R1-R2 resistor network of values 1MΩ and 240kΩ, the threshold voltage is 1.2V×(1.24M/240k) = 6.2V which is larger than 5V+0.22V(dropout)+0.7V(diode drop) ≅ 6.0V, the recommended input voltage. The low-battery indicator has no effect on the operation of the device but the user should know that the battery needs to be changed as soon as possible.

The pull-up resistor R3 pulls the open-drain output to 5V when there is no low-battery alert, and is not used in the LED operation. It is put for future versions where the LBO can be treated as a digital output. The output is by-passed with one large 10$\mu$F tantalum and one low equivalent-series-resistance (ESR) 100nF ceramic capacitors. These capacitors will supply current in case of sudden loading, when the regulator is unable to supply.

### 3.4.2 -5V (Negative) Power Supply

To generate -5V, the DC-DC inverter MAX1673 of Maxim is used. It takes the +5V generated by the regulator MAX883 as input and it generates the inverse of it,

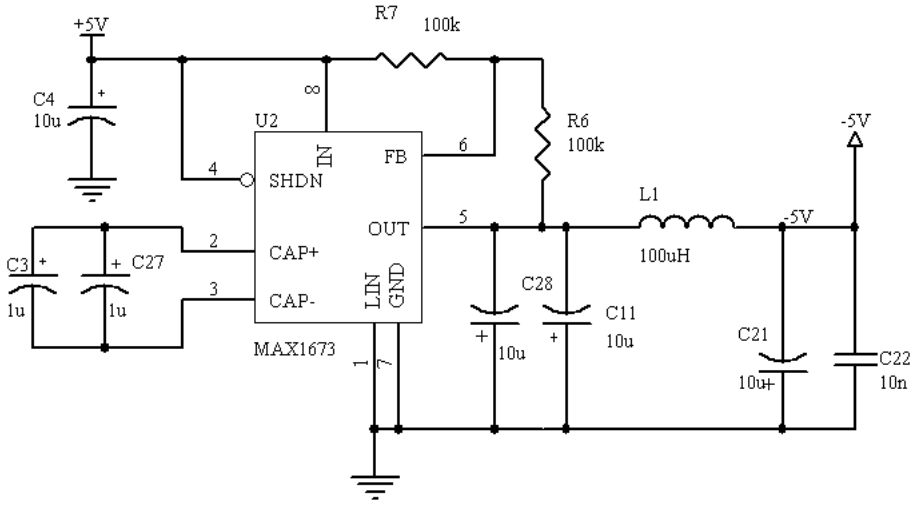


**Figure 3.13** -5V Voltage Source

namely -5V. It can supply current up to 125mA without significant ripple effect at the output. The MAX1673 operates by repetitively charging a flyer capacitor connected between the CAP+ and CAP- pins and letting it charge the output capacitor which is reverse polarized. The higher the switching frequency of the flyer capacitor from input to the output, the smaller ripples occur at the output voltage. By default MAX1673 operates at 350kHz but it is also possible to reduce the switching frequency if the current consumption is low. However, in this design the accuracy of the measurements is of higher priority. So MAX1673 is run at the default maximum frequency 350kHz. Therefore, the LIN pin, associated to the frequency selection, is connected to ground. According to the data sheet, the output voltage can be adjusted to any desired level using the equation $V_{out} = V_{in} \cdot (R6 \ / \ R7)$. To adjust the output to -5V the resistors R6 and R7 in the feedback network are selected 100k and equal to each other. As flyer capacitor, ceramic 2.2$\mu$F is recommended in the data sheet. But any capacitor larger than 1$\mu$F can be used, too. In this design two 1$\mu$F ceramic capacitors are connected in parallel to make up 2$\mu$F. For the output capacitor the recommended approach is to use a capacitor ten times larger than the flyer capacitor value according to the data sheet. In this design two 10$\mu$F tantalum capacitors are connected in parallel to make up 20$\mu$F. To minimize the ripples in the output an optional LC filter is added. With

$100\mu$H inductance and $10\mu$F capacitance values the cut-off frequency calculates to:

$$f_c = \frac{1}{2\pi\sqrt{LC}} = \frac{1}{2\pi \cdot \sqrt{100\mu H \cdot 10\mu F}} \cong 5kHz$$

It is much smaller than the switching frequency and the ripples are reduced significantly.

**Table 3.6**
Summary of the look-up table generation

| 10-bit repr. | kVp | Corr. kVp |
|---|---|---|
| 32, 64, 96, 128<br>160, 192, 224<br>256, 288, 320 | 0 | 0 |
| 352 | 121 | 0 |
| 384 | 110 | 121.7 |
| 416 | 103.6 | 111.4 |
| 448 | 98 | 102.95 |
| 480 | 93.2 | 96.15 |
| 512 | 88.9 | 90.65 |
| 544 | 85.1 | 86.1 |
| 576 | 81.7 | 82.3 |
| 608 | 78.8 | 79.1 |
| 640 | 76.15 | 76.3 |
| 672 | 73.8 | 73.8 |
| 704 | 71.7 | 71.65 |
| 736 | 69.8 | 69.7 |
| 768 | 68.05 | 67.95 |
| 800 | 66.45 | 66.35 |
| 832 | 64.95 | 64.9 |
| 864 | 63.55 | 63.5 |
| 896 | 62.2 | 62.3 |
| 928 | 61 | 61.1 |
| 960 | 59.9 | 60 |
| 992 | 58.8 | 59 |
| 1024 | 57.7 | 58 |

| Interval | Lin. Int. | Curve Fitt. | Error |
|---|---|---|---|
| 384-416 | 116.6 | 116.3 | 0.3 |
| 416-448 | 107.2 | 106.9 | 0.3 |
| 448-480 | 99.6 | 99.4 | 0.2 |
| 480-512 | 93.4 | 93.3 | 0.1 |
| 512-544 | 88.4 | 88.3 | 0.1 |
| 544-576 | 84.2 | 84.1 | 0.1 |
| 576-608 | 80.7 | 80.6 | 0.1 |
| 608-640 | 77.7 | 77.6 | 0.1 |
| 640-672 | 75.1 | 75.0 | 0.0 |
| 672-704 | 72.7 | 72.7 | 0.0 |
| 704-736 | 70.7 | 70.6 | 0.1 |
| 736-768 | 68.8 | 68.8 | 0.0 |
| 768-800 | 67.2 | 67.1 | 0.1 |
| 800-832 | 65.6 | 65.6 | 0.0 |
| 832-864 | 64.2 | 64.2 | 0.0 |
| 864-896 | 62.9 | 62.9 | 0.0 |
| 896-928 | 61.7 | 61.7 | 0.0 |
| 928-960 | 60.6 | 60.5 | 0.0 |
| 960-992 | 59.5 | 59.5 | 0.0 |
| 992-1024 | 58.5 | 58.4 | 0.1 |

# 4. MAMMOGRAPHY MODE

As this device measures the kVp of diagnostic X-ray tubes, it could be used with the mammography units as well. The operation range of the mammography tubes is usually 25-30kVp. The photons produced by this lower kVp level cannot pass through the copper filters utilized in the device and are almost completely filtered out. To overcome this problem aluminum filters of thicknesses 0.5mm and 1mm are used instead of copper. Figure 4.1 shows that the kVp-$\mu$ relation of aluminum is one-to-one and can be used to detect the kVp.

The most important point is however, as will be explained later in section 5.2, that the device should be placed such that the photodiodes are on the patient side of the mammography table, because the mammographic X-ray beam is found to be more uniform at this edge and any small change in placement of the kVp-meter does not cause any errors.

The dose measurements in Table 4.1 shows that this thickness difference (0.5mm) at these kVp levels lets the logarithm of the ratio to fall into the input range of the ADC. This means, there is no need of special adjustments in the electronic configuration. The Al filters and a second look-up table for the mammography mode suffice to add this feature to the device. A switch is put on the front panel to select the

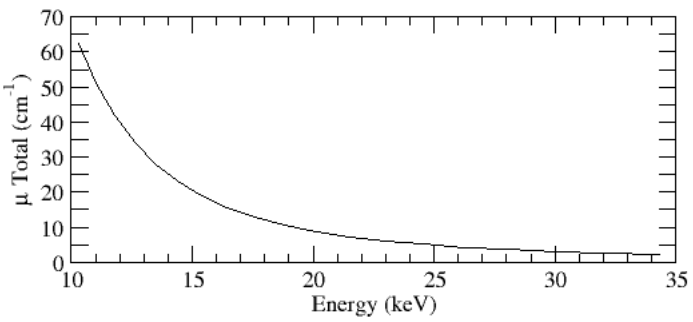


**Figure 4.1** The relation between the linear attenuation coefficient of aluminum and the incident photon energy. [1]

operation mode, between diagnostic X-ray or mammography. Accordingly, after exposure the microcontroller computes the kVp value from the look-up table of the selected mode.

## 4.1 Generation of the Look-up Table for Mammography

Similar to the diagnostic X-ray mode, mammographic dose measurements with the Al filters were used to generate the first look-up table. By computing the expected values of the input voltages of the ADC and fitting them on a smooth curve, the reference values were found and the first table was generated. It was then corrected for the actual measurement with the device. Table 4.1 and Figure 4.2 show the measured dose levels for varying kVp values in the range from 23kVp to 35 kVp, using 0.5mm Al and 1mm Al filters. The linear attenuation coefficient of Aluminum vs. kVp level is plotted in Figure 4.3.

As seen from Table 4.1 the expected voltages at the ADC input are less than the reference voltage of 2.56V and therefore measurable.

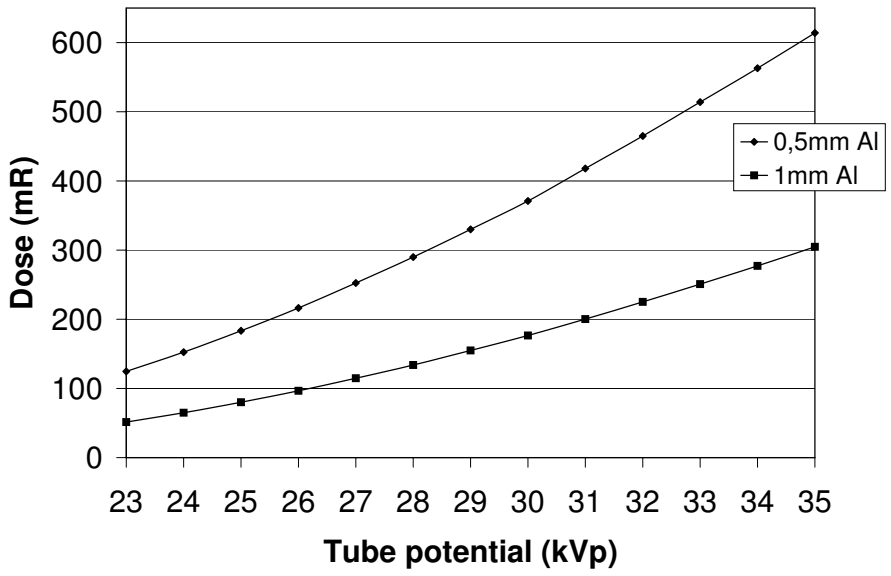


**Figure 4.2** Dose delivered vs. kVp for varying Al thicknesses.

**Table 4.1**
The doses measured by using 0.5mm ($D_1$) and 1mm Al ($D_2$) filters, the logarithms of the ratios and the expected voltage at the input of the ADC

| | **Dose (mR)** | | $log_{10}$ | **ADC input (V)** |
|---|---|---|---|---|
| **kVp** | $\mathbf{D_1}$ | $\mathbf{D_2}$ | $\mathbf{(D_1/D_2)}$ | $= 4 \times log_{10}$ |
| 23 | 124.6 | 2.42 | 0.385 | 1.538 |
| 24 | 152.5 | 2.35 | 0.371 | 1.484 |
| 25 | 183.4 | 2.29 | 0.360 | 1.439 |
| 26 | 216.4 | 2.24 | 0.350 | 1.401 |
| 27 | 252.4 | 2.20 | 0.342 | 1.369 |
| 28 | 290 | 2.17 | 0.336 | 1.342 |
| 29 | 330 | 2.13 | 0.328 | 1.314 |
| 30 | 371 | 2.10 | 0.322 | 1.290 |
| 31 | 418 | 2.09 | 0.319 | 1.278 |
| 32 | 465 | 2.06 | 0.315 | 1.260 |
| 33 | 514 | 2.05 | 0.312 | 1.247 |
| 34 | 563 | 2.03 | 0.308 | 1.231 |
| 35 | 614 | 2.01 | 0.304 | 1.217 |

The first and corrected look-up tables are given in Table 4.2.

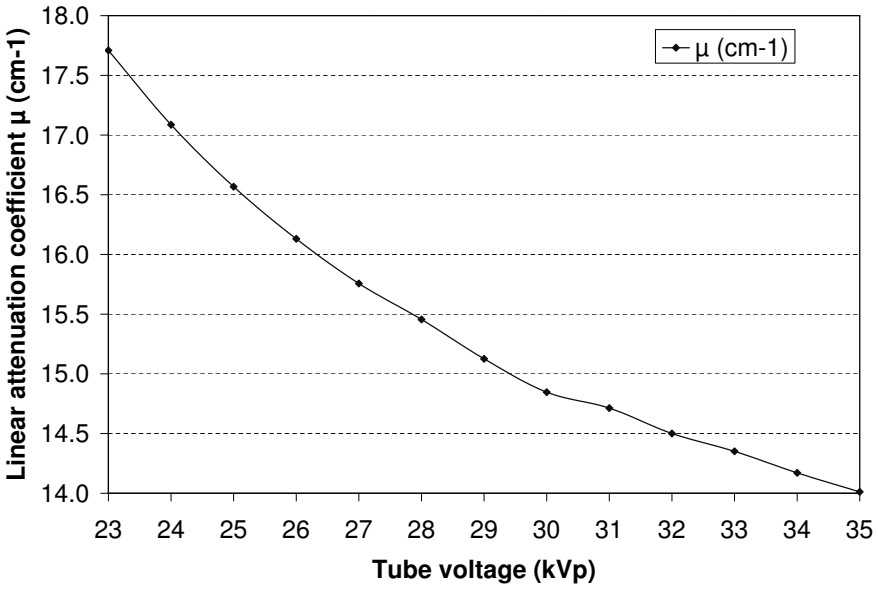


**Figure 4.3** Linear attenuation coefficient vs. kVp.

**Table 4.2**
The first and corrected look-up tables of the mammography mode

| 10-bit repr. | Init. kVp |
|---|---|
| 448 | 0 |
| 480 | 36.8 |
| 512 | 31.8 |
| 544 | 27.9 |
| 576 | 25.5 |
| 608 | 23.7 |
| 640 | 22.3 |
| 672 | 0 |

| 10-bit repr. | Corr. kVp |
|---|---|
| 352 | 0 |
| 384 | 35.6 |
| 416 | 32.7 |
| 448 | 30.0 |
| 480 | 27.5 |
| 512 | 25.2 |
| 544 | 23.2 |
| 576 | 0 |

# 5. RESULTS

## 5.1 Diagnostic Radiography Mode

After calibration, namely correction of the look-up table the device measures with a very good accuracy. Table 5.1 shows the measurements conducted after calibration of the device. Since the device was calibrated for tube distance of 86cm, the values of 86cm distance are closer to the set kVp value. Another measurement was taken from 50 cm tube distance for comparison. The table shows that the measurements deviated from the true values. This fact emphasizes the dependency of the accuracy to the measurement conditions. At 86cm the device works well but for 50cm not. This problem does not apply for the mammography mode, since the table-tube distance is fixed. Once calibrated, the device is expected to work fine. Another point is the closeness of the measurement results at 86cm. This proves the reliability of both the X-ray tube and this device. At the same set conditions, almost same results were obtained.

For the resolution, 0.1kVp is achieved on the most part of the kVp range. At kVp levels higher than 90kVp it is 0.2kVp and for higher than 110kVp, it is 0.3kVp. However, this does not cause a significant error on the measurements. According to the AAPM (The American Association of Physicists in Medicine) standards, an X-ray unit passes the kVp accuracy test for an error range $\pm 5\%$ and the kVp-meters are treated as calibrated for error ranges $\pm 1\%$ [6].

To test the dependency of the measurements on mAs, several measurements were conducted at constant kVp and varying mAs. There were no deviations in the results that can be reported. It can be concluded, this device measures independent of mAs setting.

To test the dependency of the accuracy on the positioning, namely to check whether the results deviate when the device is not put directly to the center of the

**Table 5.1**
The kVp measurements after calibration of the device. SID=86cm.

| | Measurements | | Error (kVp) |
|---|---|---|---|
| **Set kVp** | **50cm** | **86cm *** | **due to SID** |
| 60 | 58.9 | 60.0 | 1.1 |
| 61.5 | 60.3 | 61.5 | 1.2 |
| 63 | 61.6 | 62.9 | 1.3 |
| 64.5 | 63.2 | 64.5 | 1.3 |
| 66 | 64.4 | 65.8 | 1.4 |
| 70 | 68.2 | 69.9 | 1.7 |
| 73 | 70.8 | 72.8 | 2.0 |
| 75 | 72.6 | 74.8 | 2.2 |
| 77 | 74.4 | 76.8 | 2.4 |
| 79 | 76.0 | 78.7 | 2.7 |
| 81 | 77.7 | 80.7 | 3.0 |
| 85 | 81.0 | 84.6 | 3.6 |
| 90 | 85.0 | 89.6 | 4.6 |
| 96 | 89.9 | 95.3 | 5.4 |
| 102 | 94.9 | 100.2 | 5.3 |
| 109 | 100.4 | 106.4 | 6.0 |
| 113 | 103.5 | 110.1 | 6.6 |
| 117 | 106.9 | 113.6 | 6.7 |
| 121 | 109.8 | 117.2 | 7.4 |

* Average of 3 readings

beam, the device was moved 7 cm to each direction. Again there were no deviations that can be reported. But missing the center more than this, may result in inaccurate measurements.

### 5.1.1 Accuracy

To test the accuracy the kVp is measured in the whole range. The measurement results are given in Table 5.2. As seen the deviation is less than 0.3% everywhere in

the measurement range once calibrated.

**Table 5.2**
The kVp measurements for accuracy and the percent errors.

| set kVp | kvp-meter reading | Error % |
|---|---|---|
| 60 | 60.0 | 0.1 |
| 61.5 | 61.5 | 0.0 |
| 63 | 62.9 | 0.1 |
| 64.5 | 64.5 | 0.1 |
| 66 | 65.8 | 0.3 |
| 70 | 69.9 | 0.2 |
| 73 | 72.8 | 0.2 |
| 75 | 74.8 | 0.3 |
| 77 | 76.8 | 0.3 |
| 79 | 78.7 | 0.4 |
| 81 | 80.7 | 0.4 |
| 85 | 84.6 | 0.4 |
| 90 | 88.4 | 1.8 |
| 96 | 94.2 | 1.9 |
| 102 | 99.8 | 2.2 |
| 109 | 106.5 | 2.3 |
| 117 | 113.6 | 2.9 |
| 121 | 117.4 | 3.0 |

### 5.1.2 Precision

To test the precision, the kVp was set to 81kVp and measured repeatedly. The measurement results are given in Table 5.3. The ratio of standard deviation to the kVp level is 0.08% which is below the 1% limit [13].

**Table 5.3**
The kVp measurements for precision.

| Measurement | kVp reading |
|---|---|
| 1 | 80.7 |
| 2 | 80.6 |
| 3 | 80.7 |
| 4 | 80.7 |
| 5 | 80.7 |
| 6 | 80.7 |
| 7 | 80.8 |
| 8 | 80.8 |

| | |
|---|---|
| Average | 80.713 |
| STD | 0.064 |
| STD / Average | 0.08% |

### 5.1.3 Comparison with a calibrated commercial kVp-meter

The kVp-meter readings are compared with the measurements of a factory calibrated commercial kVp-meter, Victoreen 07-743. The device is not calibrated against this calibrated one but the measurements on three different X-ray tubes agree in ±5% as given in Table 5.4.

## 5.2 Mammography Mode

The results of the mammography mode are as accurate as those of the diagnostic X-ray mode. The only point is, that the device should be placed such that the photodiodes are on the patient side of the mammography table, namely backward, because the mammographic X-ray beam is found to be more uniform at this edge and any small change in placement of the kVp-meter does not cause any errors. This fact arises a discomfort for the user in reading the display, since it is faced to the mammography

**Table 5.4**
The kVp-meter readings compared with a calibrated kVp-meter (Victoreen 07-743).

| **set kVp** | **Siemens Multix Compact K** | | **Siemens Multix K** | | **Imago Europa 2TS** | |
|---|---|---|---|---|---|---|
| | kVp-meter | 07-743 | kVp-meter | 07-743 | kVp-meter | 07-743 |
| **60** | | | | | 72.8 | 76.8 |
| **66** | 65.8 | 64.5 | 66.4 | 64.8 | | |
| **70** | 69.9 | 68.2 | 70.3 | 68.4 | 81.9 | 83.5 |
| **75** | 74.8 | 72.4 | 75.4 | 72.7 | | |
| **80** | | | | | 93.6 | 88.5 |
| **81** | 80.7 | 76.7 | 81.3 | 77 | | |
| **90** | | | | | 103.7 | 100.7 |

unit.

Table 5.5 shows the measurement results after calibration. There are no errors to be reported due to mAs variations. Measurements with mAs settings from 20mAs up to 50mAs resulted in the same kVp value.

## 5.3 Reliability of the Measurements

This device is noninvasive, therefore does not directly measure kVp, but rather measures the beam hardness and relates it to the actual kilovoltage used under the calibration conditions. The variations in beam hardness between different X-ray units operated at the same tube potential may lead to erroneous results. Moreover, noise and the scattered photons may also affect the accuracy of the measurements.

**Table 5.5**
The kVp measurements in mammography mode after calibration of the device.

| set kVp | Measured kVp | % Error |
|---|---|---|
| 23 | 23.0 | 0.0 |
| 24 | 24.0 | 0.0 |
| 25 | 25.0 | 0.0 |
| 26 | 26.0 | 0.0 |
| 27 | 26.9 | 0.4 |
| 28 | 27.9 | 0.4 |
| 29 | 28.9 | 0.4 |
| 30 | 29.9 | 0.4 |
| 31 | 30.8 | 0.6 |
| 32 | 31.8 | 0.6 |
| 33 | 32.8 | 0.6 |
| 34 | 33.7 | 0.9 |

### 5.3.1 Noise

One of the factors affecting the stability of the measurements is the noise. Sample averaging, low-pass filters at the input of the ADC and at the ADC power supply, by-passing the reference voltage to ground are the methods used to minimize the noise and interference problems.

### 5.3.2 Scattered Photons

A second important factor is the photons scattered from the environment, namely the device plastic box or the radiographic table, etc. that may hit the photodiodes and affect accuracy of the measurements. To prevent these secondary photons from reaching the photodiodes, they are put in a lead case. Only the top of the case is open and only the photons from the primary beam, namely from the X-ray tube can reach the photodiodes. To prevent photons that pass through the photodiodes and that may be scattered by the bottom of the box or the patient table reaching the pho-

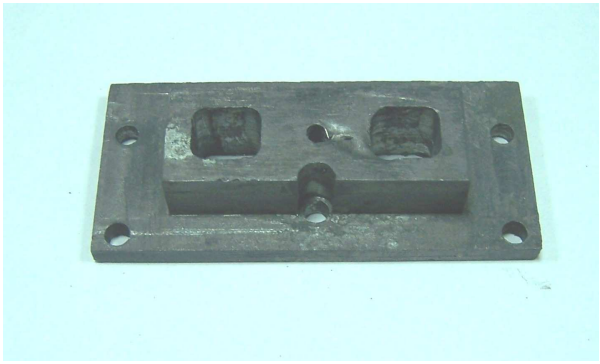

**Figure 5.1** The lead case for photodiodes

todiodes from bottom and affecting the measurements the whole inner bottom surface of the box is covered with a sheet of lead. Lead is expected to absorb any incident X-ray photon. Figure 5.1 and Figure 5.2 show the lead case and the lead sheets used to cover the inner surface, respectively.

### 5.3.3 Dependency on the Beam Hardness

The output spectrum of the X-ray tubes namely the hardness of the X-ray beam produced at the same tube potential, may differ from device to device. This is observable as the peak relative intensity in the spectrum. As seen from Figure 5.3, the beam is not monochromatic. Therefore, the measurement is actually not the $\mu$ for the highest energy photons, rather a $\mu$ that represents the mean energy level of the photons. Then, according to the look-up table the corresponding kVp is found and displayed. The peaks due to the characteristic radiations are not of prime importance, since their contribution to the spectrum can be ignored.

If, the device in reality determines where the peak is and the outputs of different tubes may vary, a correction should be applied when the quality of the tube to be measured is different than reference tube. The point here is, what is the measure for the quality. The answer is the half value layer (HVL) of the tube. HVL means the thickness of the filter that can halve the intensity of the incident beam and is usually around 3mm Al.

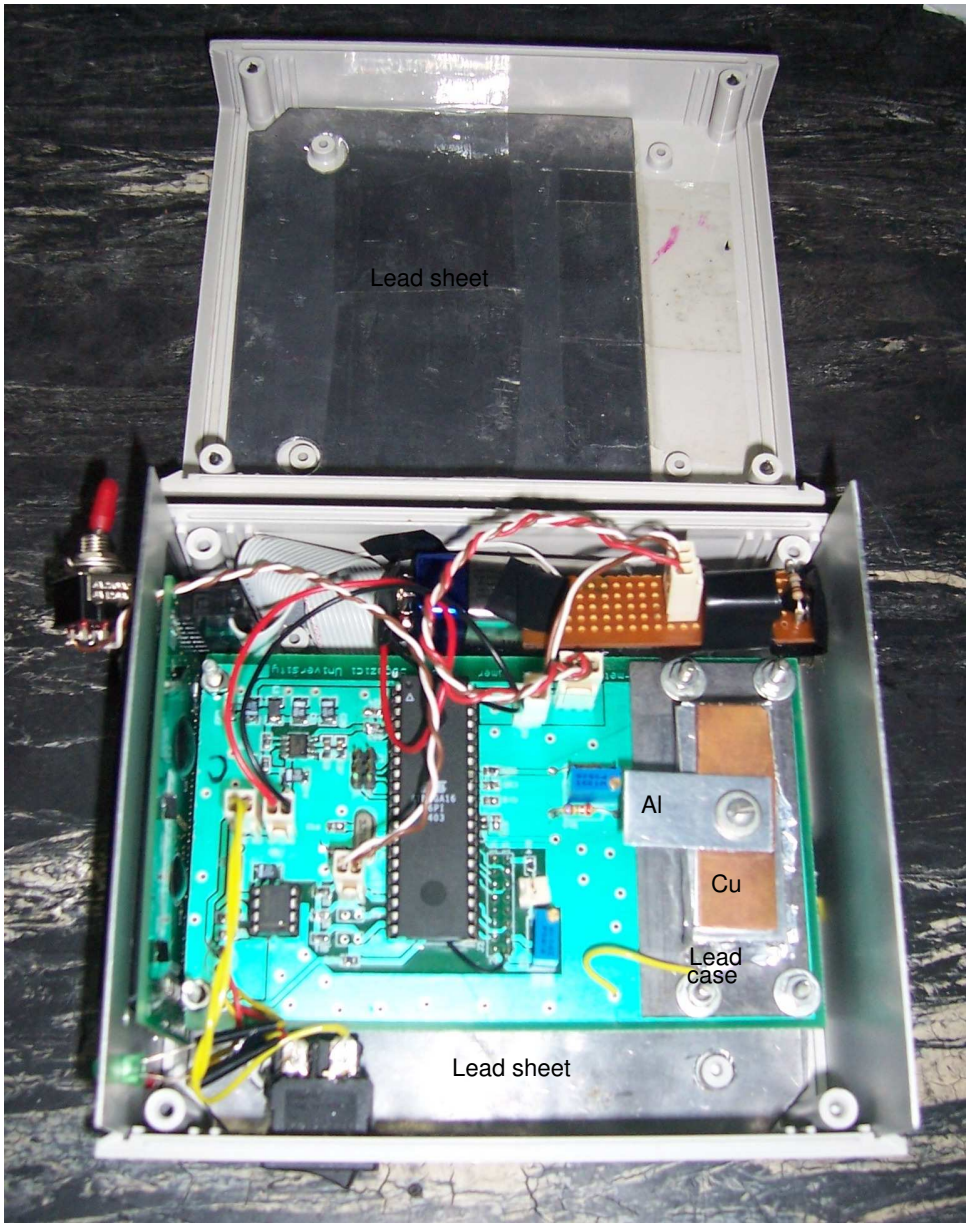


**Figure 5.2** View on the inside of the device

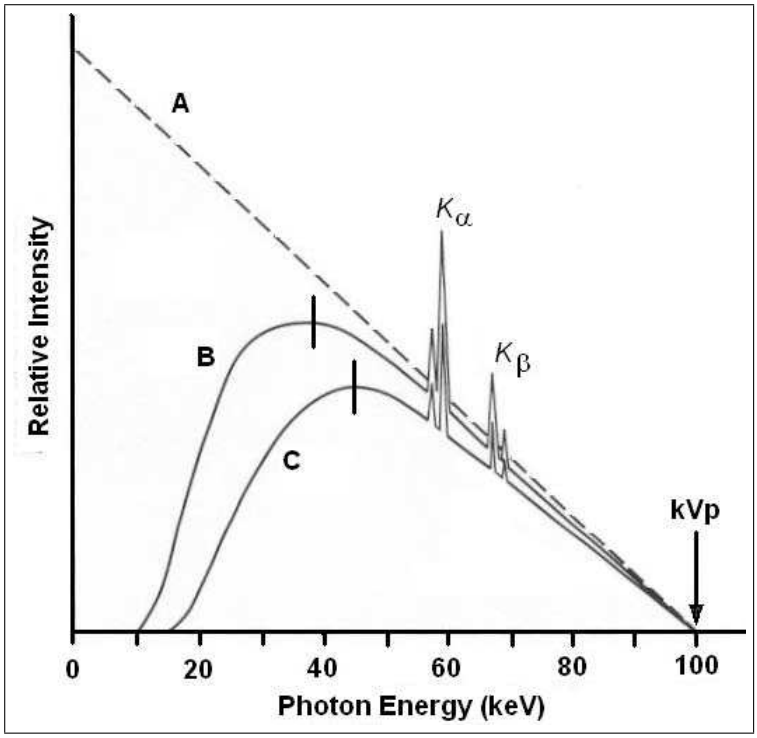


**Figure 5.3** **A)** The theoretical spectrum of the generated X-ray photons inside the anode. **B)** The spectrum of the photons that are left after being filtered inside the tungsten target. **C)** The spectrum of the beam after additional filtration.

The more filtering is applied on the X-ray beam, the more the lower energy photons are eliminated and the more the peak of the spectrum shifts to right. This is called beam hardening, because the penetration power of the beam increases although the intensity in total decreases. The decrease in intensity does not cause any problem in measurement, because according to Equation 2.7 the intensity of the incident beam has no effect. Figure 5.3 shows how the peak shifts.

Since after every filtration the penetration power increases, namely only high energy photons survive, a thicker filter is needed to halve the intensity and the shifting of the spectrum peak slows down.

To minimize the error caused by the HVL differences, additional 2mm Al filter is used in this device. 2mm Al eliminates most of the lower energy photons, shifts the spectrum to right and approximates the spectra of different tubes to each other. Then, it is expected that the device works with less dependency on the tube quality.

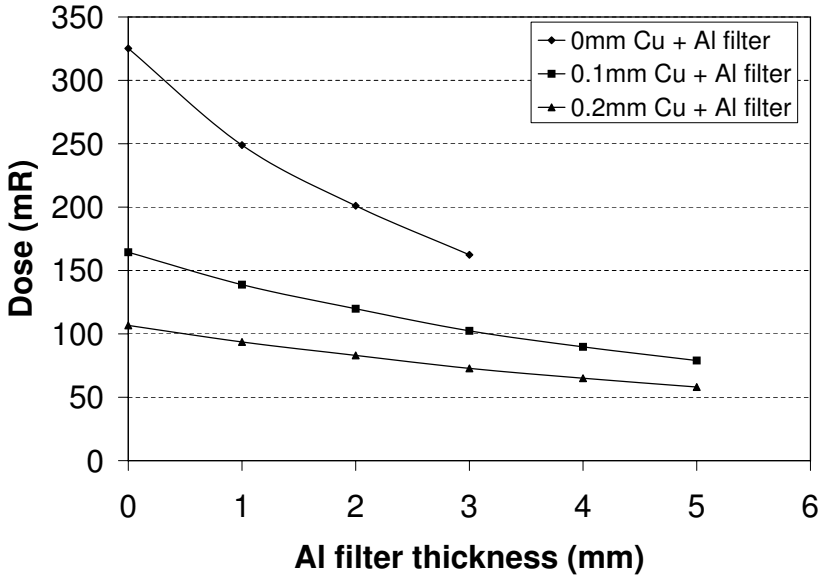


**Figure 5.4** Measured doses with varying Al filter thicknesses.

To obtain an X-ray tube with different (in this case higher) HVL's, the beam was filtered with additional 0.1mm and 0.2mm Cu sheets. Using the dosimeter the HVL for each case is found as in Figure 5.4. So, the HVL dependency can be tested for 3 different HVL's. The results are given in Table 5.6. The last two columns give the errors due to HVL differences. Figure 5.5 gives an graphical representation of the errors with respect to the kVp level.

**Table 5.6**
The kVp measurements with different HVL's. $HVL_1$=3mm Al; $HVL_2$=4.6mm Al; $HVL_3$=5.6mm Al

| | **kVp-meter Readings** | | |
|---|---|---|---|
| **set kVp** | **$HVL_1$** | **$HVL_2$** | **$HVL_3$** |
| **60** | 60.4 | 61.5 | 62.4 |
| **63** | 63.4 | 64.6 | 65.5 |
| **66** | 66.4 | 67.7 | 68.7 |
| **70** | 70.3 | 71.8 | 73.0 |
| **75** | 75.4 | 77.0 | 78.6 |
| **81** | 81.3 | 83.1 | 85.0 |
| **85** | 85.0 | 87.5 | 89.5 |
| **90** | 89.8 | 92.7 | 95.3 |
| **99** | 99.1 | 102.3 | 105.6 |
| **109** | 109.3 | 113.6 | 117.5 |

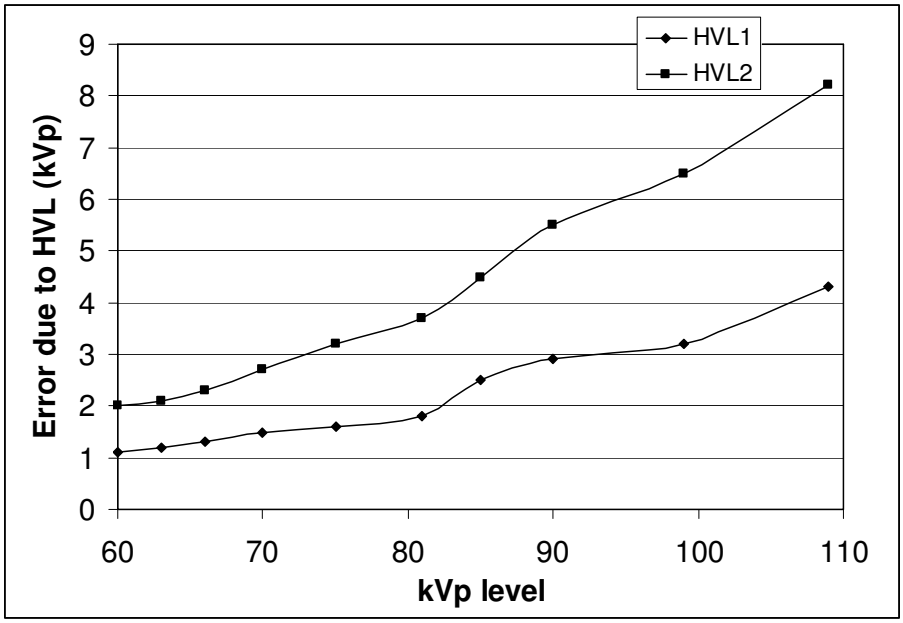


**Figure 5.5** Errors in kVp-meter readings due to HVL differences with respect to kVp level. $HVL_2$=4.6mm Al; $HVL_3$=5.6mm Al.

# 6. CONCLUSION

An accurate and reliable device is designed and built. This device works very accurately if the measurement conditions are the same as those at calibration. For ease of use, the device can be recalibrated to use at 50cm or 40cm tube distance. The timer is also thought to be very accurate since the accuracy of the crystal is given to be within 100ppm.

In the future, a new kVp-meter with 12-bit ADC and 4 photodiodes can be implemented. 12-bit ADC will allow the device 0.1kVp resolution everywhere in the covered kVp-range. 2 out of the 4 photodiodes can have the same function as those used in this device. The other 2 may be filtered with Al filters only and placed very close to the front panel, to avoid the unfavorable backward placement of the device and the discomfort in reading the display.

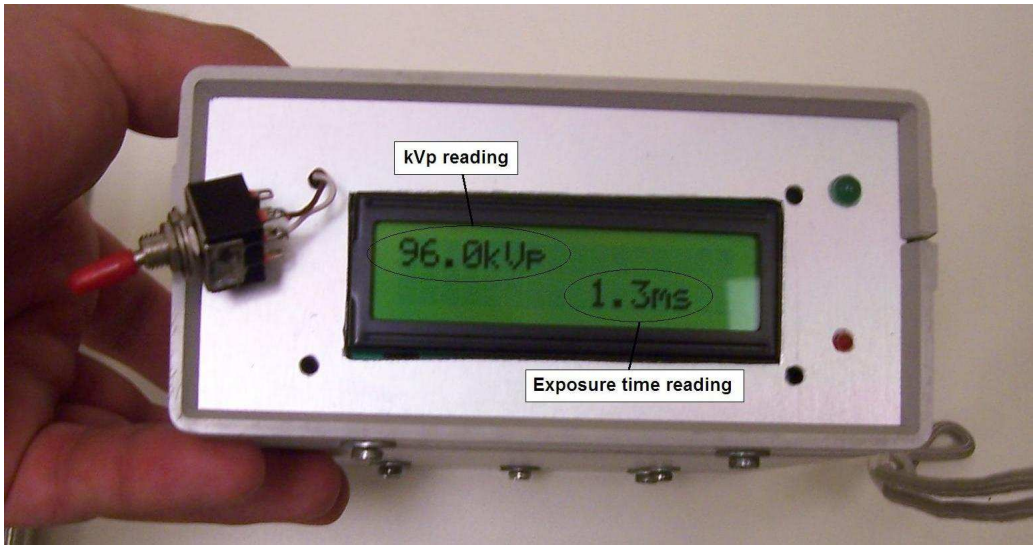


**Figure 6.1** The front view of the device.

# REFERENCES


1. "National Institute of Standards and Technology (NIST), Physics Laboratory." X-ray Form Factor, Attenuation nd Scattering Tables.

2. "Georgia State Universtiy Department of Physics and Astronomy website." http://hyperphysics.phy-astr.gsu.edu.

3. Wolbarst, A. B., *Physics of Radiology*, Medical Physics Publishing, 2 ed., 2000.

4. "Log101: Precision logarithmic and log ratio amplifier." Data sheet.

5. Anderson, D. W., G. J. Moore, and P. D. Lester, "Absolute kvp calibration using characteristic x-ray yields," *Med Phys.*, Vol. 13, no. 5, pp. 663–6, 1986.

6. AAPM, "Quality control in diagnostic radiology," 2002. Diagnostic X-ray Imaging Committee Task Group 12.

7. Gilbertson, J. D., and A. G. Fingerhut, "Standardization of diagnostic x-ray generators," *Radiology*, Vol. 93, no. 5, pp. 1033–6, 1969.

8. Q.A. Collectible, "kVp Measurements," Conference of Radiation Control Program Directors, Inc., 1994.

9. Kunzel, R., S. B. Herdade, R. A. Terini, and P. R. Costa, "X-ray spectroscopy in mammography with a silicon pin photodiode with application to the measurement of tube voltage," *Med Phys.*, Vol. 31, no. 11, pp. 2996–3003, 2004.

10. Jacobson, A. F., J. R. Cameron, M. P. Siedband, and J. Wagner, "Test cassette for measuring peak tube potential of diagnostic x-ray machines," *Med Phys.*, Vol. 3, no. 1, 1976.

11. Ranallo, F. N., S. J. Goetsch, L. A. DeWerd, M. M. Liss, C. Borras, C. White, J. Barton, T. Mian, S. Malik, and S. Wolff, "Calibration and use of the wisconsin kvp test cassette," *Med Phys.*, Vol. 15, no. 5, pp. 768–772, 1988.

12. Hendee, W. R., and E. R. Ritenour, *Medical Imaging Physics*, Wiley-Liss, 4 ed., 2002.

13. AAPM, "Basic quality control in diagnostic radiology," 1977. Report 4.